Inorganic Chemistry

Article

pubs.acs.org/IC

[1.1]Ferrocenophanes and Bis(ferrocenyl) Species with Aluminum and Gallium as Bridging Elements: Synthesis, Characterization, and Electrochemical Studies

Bidraha Bagh,[†] Nora C. Breit,[†] Klaus Harms,[§] Gabriele Schatte,[‡] Ian J. Burgess,[†] Holger Braunschweig,[∥] and Jens Müller*,[†]

[†]Department of Chemistry and [‡]Saskatchewan Structural Sciences Centre, University of Saskatchewan, 110 Science Place, Saskatoon, Saskatchewan S7N 5C9, Canada

[§]Fachbereich Chemie, Philipps-Universität Marburg, Hans-Meerwein-Strasse, 35032 Marburg, Germany

[∥]Institut für Anorganische Chemie, Julius-Maximilians-Universität Würzburg, Am Hubland, 97074 Würzburg, Germany

Supporting Information

ABSTRACT: Salt-metathesis reactions between dilithioferrocene ($Li_2fc \cdot 2/3tmeda$) and intramolecularly coordinated aluminum and gallium species $RECl_2$ [R = 5-Me_3Si-2-(Me_2NCH_2)C_6H_3; E = Al (**2a**), Ga (**2b**); and R = (2-C_5H_4N)Me_2SiCH_2; E = Al (**3a**), Ga (**3b**)] gave respective [1.1]ferrocenophanes ([1.1]FCPs). Those obtained from **2a** and **2b**, respectively, were isolated as analytically pure compounds and fully characterized including single-crystal X-ray structure determinations [**4a** (Al): 43%; **4b** (Ga): 47%]. Bis(ferrocenyl) compounds of the type $REFc_2$ [R = 5-Me_3Si-2-(Me_2NCH_2)C_6H_3; E = Al (**5a**), Ga (**5b**); and R = (2-C_5H_4N)Me_2SiCH_2; E = Al (**6a**), Ga (**6b**)] and R_2SiFc_2 [R = Me ($\mathbf{7^{Me}}$); Et ($\mathbf{7^{Et}}$)] were prepared, starting from respective element dichlorides and lithioferrocene (LiFc). Molecular structures of **6a**, $\mathbf{7^{Me}}$, and $\mathbf{7^{Et}}$ were solved by single-crystal X-ray analyses. One of the two Fc moieties of **6a** was bent toward the open coordination site of the aluminum atom. The measured dip angles α^* of the two independent molecules in the asymmetric unit were 11.9(5) and 13.3(5)°, respectively. The redox behavior of [1.1]FCPs **4** and bis(ferrocenyl) species **5**, **6**, **7**, and (Mamx)EFc_2 [Mamx = 2,4-$t$$Bu_2$-6-($Me_2NCH_2$)$C_6H_2$; E = Al (**8a**), Ga (**8b**)] were investigated with cyclic voltammetry. While all gallium and silicon compounds gave meaningful and interpretable data, all aluminum compounds were problematic with the exception of **8a**. Aluminum species, compared to respective gallium species, are more sensitive and, presumably, fluoride ions or residual water from the electrolyte and solvent are causing degradation. The splitting between the formal potentials for bis(ferrocenyl) species was significantly smaller (**5b**, **6b**, and **8b**: $\Delta E^{\circ\prime}$ = 0.138−0.159 V) than that of the [1.1]FCP **4b** ($\Delta E^{\circ\prime}$ = 0.309 V). These results were explained by assuming an electrostatic interaction between the two iron centers; differences between bis(ferrocenyl) species and [1.1]FCPs are likely due to a more effective solvation of Fe-containing moieties in the more flexible bis(ferrocenyl) species.

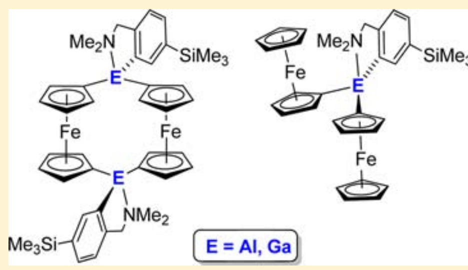

■ INTRODUCTION

[n]Ferrocenophanes ([n]FCPs; Chart 1) with one or two-atom bridges (n = 1, 2) with significantly tilted Cp rings (α angles above ca. 14°) often show a propensity toward ring-opening polymerization (ROP) resulting in poly(ferrocene)s.[1] This area of chemistry began with the synthesis of a [2]FCP equipped with a C_2Me_4 bridge, which was the first strained sandwich compound published in 1960.[2] After the first [1]FCPs (ER_x = $SiMe_2$, $SiPh_2$; Chart 1) had been described in 1975,[3] it took more than 15 years before this area of polymer chemistry started to blossom with the discovery that silicon-bridged [1]FCPs yield high-molecular-weight polymers through thermal ROP.[4] To date, silicon-bridged [1]FCPs form the most prominent class of strained sandwich compounds and serve as excellent precursors for metallopolymers.[1,5]

Chart 1

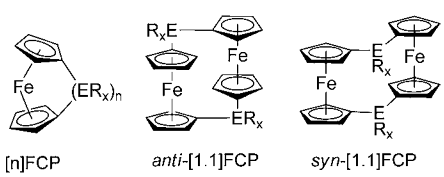

[1.1]Ferrocenophanes ([1.1]FCPs; Chart 1) are unstrained dimers of [1]FCPs and had been investigated as early as 1956.[6] Today, the large class of [1.1]FCPs consists of examples with a variety of bridging moieties ER_x (Chart 1; E = B,[7] Al,[8] Ga,[8b,9] In,[8b,10] Si,[11] Sn,[12] Pb,[13] P,[14] As,[15] S,[16] Zn,[17] and Hg[18]). Recently, we developed a methodology for the preparation of unsymmetric [1.1]FCPs, compounds with two different single-atom bridges, and realized the element combinations of Si/Sn and Si/Ga, respectively.[19] In addition, cyclic species with four

Received: August 13, 2012
Published: September 25, 2012

   dx.doi.org/10.1021/ic301777y | *Inorg. Chem.* 2012, 51, 11155−11167

ferrocenediyl units [fc = $(C_5H_4)_2Fe$] were isolated, while, in some cases, macrocycles with up to 20 fc units were detected by MALDI-TOF mass spectrometry.[19] Macrocyclic ferrocenophanes with multiple fc moieties are known, but significantly rarer compared to the large class of [1.1]FCPs.[11f,14b,20] To the best of our knowledge, the largest isolated FCPs contained seven ferrocene moieties,[20e,i,l] while [1^n]FCPs[21] with $n > 40$ are the largest macrocycles of this type described in literature (detected by MALDI-TOF mass spectrometry).[20l]

Despite the impressive progress made during the past two decades to use strained sandwich compounds for new metallopolymers, there is still a need to develop new monomers, in particular, species that can be polymerized in a living fashion. Since 2004, we prepared aluminum- and gallium-bridged sandwich compounds and explored their polymerizability.[22] Our first generation of these species had been equipped with bulky, intramolecularly coordinating ligand at the group 13 elements (e.g., Pytsi; Chart 2). However, attempts

Chart 2. Intramolecularly Coordinating Ligands

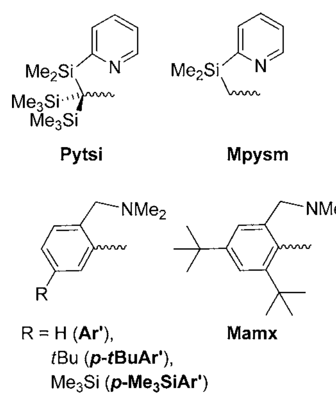

to polymerize [1]FCPs or their ruthenium counterparts ([1]RCPs) either failed or resulted in sluggish polymerizations,[22d] indicating that the bulkiness of the stabilizing ligands was hindering the ROP. We discovered that the use of the related, but slimmer 2-[(dimethylamino)methyl]phenyl ligand (Ar′; Chart 2) in respective salt-metathesis reactions of $Li_2fc \cdot 2/3tmeda$ and aluminum or gallium dichlorides $Ar'ECl_2$ resulted in [1.1]FCPs (**1a** and **1b**; Chart 3) instead of the

Chart 3. Known [1.1]FCPs 1a and 1b

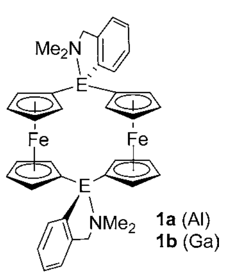

strained [1]FCPs.[8a,b] The use of $(Mamx)ECl_2$ species (E = Al, Ga; Chart 2), equipped with a ligand of intermediate bulkiness, led to [1]FCPs and [1]RCPs, which were surprisingly reactive and ROP occurred already in reaction mixtures.[22a,c] The bulkiness of the stabilizing ligand at the group 13 element plays a key role for the accessibility of strained sandwich compounds as well as for their polymerizability.

Within this report, we describe new aluminum and gallium dichlorides, $(Mpysm)ECl_2$ and $(p\text{-}Me_3SiAr')ECl_2$ (Chart 2), and their utilization in salt metathesis reactions with dilithioferrocene ($Li_2fc \cdot 2/3tmeda$) and lithioferrocene (LiFc). We intended to compare Fe−Fe interactions in [1.1]FCPs with those in the related bis(ferrocenyl) compounds $(Mpysm)EFc_2$ and $(p\text{-}Me_3SiAr')EFc_2$. For this study, we equipped the Ar′ ligand with a $SiMe_3$ group in *para* position (p-Me_3SiAr'; Chart 2) to access [1.1]FCPs, like the known species **1a** and **1b** (Chart 3), but with an improved solubility in organic solvents. Such a tactic had been successfully applied for [1.1]-metallacyclophanes through the use of the *p*-*t*BuAr′ ligand (Chart 2).[23] The Mpysm ligand[24] was applied because of its relation to the Pytsi ligand (Chart 2).

RESULT AND DISCUSSION

Synthesis of Aluminum and Gallium Dichlorides. Scheme 1 illustrates the preparation of new intramolecularly

Scheme 1

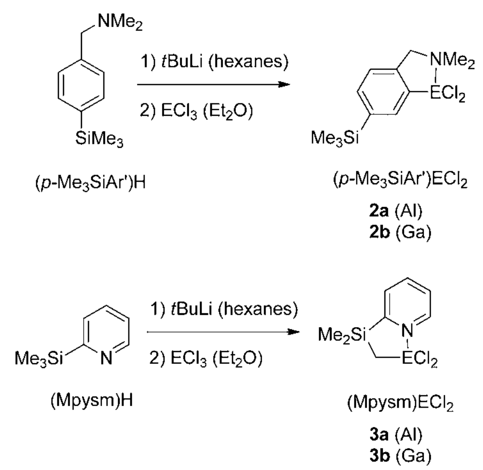

coordinated aluminum and gallium dichlorides, which were isolated in yields between 47 and 73%.[25] As expected, NMR spectra of all four species showed a signal pattern consistent with C_s symmetric molecules.

We were interested to compare the structures of the halides equipped with the Mpysm ligand with those of the respective $(Pytsi)ECl_2$ species. Therefore, the molecular structure of **3b** was determined by single-crystals X-ray analysis (Figure 1, Table 1). The molecular structure of **3b** is very similar to that of the related dihalide $(Pytsi)GaCl_2$.[22g] The geometry at gallium is distorted tetrahedral in both species, and the bite angles are nearly identical (C7−Ga1−N1 = 98.79(7) (**3b**), 98.03(9)° [$(Pytsi)GaCl_2$]). The Ga−N bond lengths of 2.0126(16) Å (**3b**) is within three esd's identical to that in $(Pytsi)GaCl_2$ [Ga−N = 2.004(2) Å]. The other three covalent bonds around the Ga atom in **3b** are only slightly different, with the largest difference of 0.04 Å found for the Ga−C bonds [**3b**: 1.949(2) Å; $(Pytsi)GaCl_2$: 1.988(2) Å]. For a better comparison of the geometries of both species, the coordination could be described as trigonal pyramidal with C7, Cl1, and Cl2 at the base and N1 at the tip of the pyramid. The pyramid of **3b** is more acute compared with that of $(Pytsi)GaCl_2$, which can be illustrated with the sum of the three angles C7−Ga1−Cl2, C7−Ga1−Cl1, Cl1−Ga1−Cl2. Whereas this sum for **3b** of 335.4° is close to the expected value for a tetrahedral

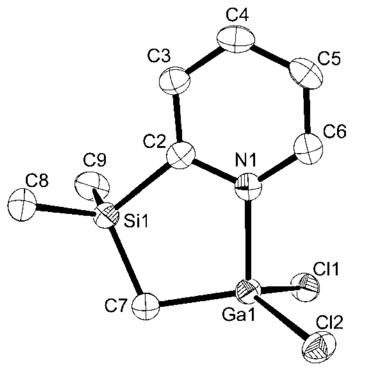

Figure 1. Molecular structure of **3b** with thermal ellipsoids at the 50% probability level. Hydrogen atoms are omitted for clarity. Selected atom−atom distances [Å] and bond angles [deg] for **3b**: Ga1−N1 = 2.0126(16), Ga1−C7 = 1.949(2), Ga1−Cl1 = 2.2024(5), Ga1−Cl2 = 2.1927(6), C7−Ga1−Cl1 = 118.10(7), C7−Ga1−Cl2 = 121.94(7), C7−Ga1−N1 = 98.79(7), N1−Ga1−Cl1 = 103.42(5), N1−Ga1−Cl2 = 102.16(5), Cl1−Ga1−Cl2 = 108.54(2).

coordination, that in (Pytsi)$GaCl_2$[22g] of 350.0° is closer to the expected value of a trigonal-planar coordination at the base. This difference is probably due to the steric requirements of the two $SiMe_3$ groups in (Pytsi)$GaCl_2$ which results in a widening of the two C−Ga−Cl angles [121.49(8) and 124.77(8)°] compared with those in **3b** [103.42(5) and 102.16(5)°].

Synthesis of Aluminum- and Gallium-bridged [1.1]-Ferrocenophanes. With the heavier group-13-element dichlorides in hand, the reactivity toward $Li_2fc·2/3tmeda$ was explored. Following standard procedures, the two [1.1]-ferrocenophanes **4a** and **4b**, equipped with the *p*-Me_3SiAr' ligand (Chart 2), were synthesized and isolated in moderate yields (**4a**: 43%; **4b**: 47%; Scheme 2).

Scheme 2

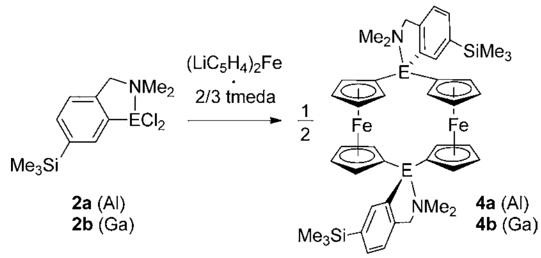

Both species gave single crystals of suitable quality for structural determinations from thf solution at ca. −25 °C (Figure 2, Table 1). Species **4a** and **4b** are isostructural to each other and to the known [1.1]FCPs (**1a** and **1b**; Chart 3), where the $SiMe_3$ group is absent (space group $P2_1/c$). As expected, both species crystallize as *anti*-isomers (Chart 1) and their bond lengths and angles are unremarkable and very similar to those of the known species **1a** and **1b** (Chart 3).[8a,b] For example, the Fe···Fe distances of the aluminum [5.3946(8) (**4a**); 5.443 Å (**1a**)[8a]] and gallium species [5.4277(8) (**4b**); 5.462 Å (**1b**)[8b]] are all in the narrow range of 5.395−5.462 Å.

NMR data of **4a** and **4b** are very similar to that of the known species **1a** and **1b**.[8a,b] The most indicative area in ^1H NMR spectra is the Cp range, where both species (**4a**, **4b**) show only four signals, which can be explained by the presence of time-averaged C_{2h} symmetrical species.[26] This means that both species have similar structures in solution as in the solid state (C_i point group symmetry), if one takes into account that the five-membered rings of the coordinated *p*-Me_3SiAr' will invert fast in solution.[27]

The motivation to use the *p*-Me_3SiAr' ligand instead of the Ar′ ligand was to increase the solubility of the targeted [1.1]FCPs. Such a tactic had worked for [1.1]chrom-

Table 1. Crystal and Structural Refinement Data for Compounds 3b, 4a, and 4b

	3b	4a·2thf	4b·2thf
empirical formula	$C_8H_{12}Cl_2GaNSi$	$C_{52}H_{72}Al_2Fe_2N_2O_2Si_2$	$C_{52}H_{72}Ga_2Fe_2N_2O_2Si_2$
fw	290.90	978.96	1064.44
cryst. size/mm^3	0.31 × 0.20 × 0.08	0.09 × 0.06 × 0.06	0.10 × 0.09 × 0.07
cryst. system, space group	monoclinic, C2/*c*	monoclinic, $P2_1/c$	monoclinic, $P2_1/c$
Z	8	2	2
a/Å	24.8987 (15)	11.1745(3)	11.1015(3)
b/Å	8.4418 (3)	19.2904(5)	19.3907(6)
c/Å	11.9599 (7)	12.1908(4)	12.2577(4)
α/deg	90	90	90
β/deg	104.633(5)	106.1100(17)	106.5540(10)
γ/deg	90	90	90
volume/Å^3	2432.3(2)	2524.66(13)	2529.30(13)
ρ_{calc}/mg m^{-3}	1.589	1.288	1.398
temperature/K	100	173(2)	173(2)
μ_{calc}./ mm^{-1}	2.76	5.708	6.484
θ range/deg	1.69−26.69	4.12−66.63	4.15−66.90
reflns collected/unique	15220/2577	17246/4373	17093/4369
absorption correction	multiscan	multiscan	multiscan
data/restraints/params	2577/0/120	4373/178/331	4369/178/331
goodness-of-fit	0.917	1.015	1.039
R_1 [$I > 2\sigma(I)$]^a	0.0218	0.0410	0.0418
wR_2 (all data)^a	0.0501	0.1156	0.1197
largest diff. peak and hole, $\Delta\rho_{elect}$/e Å^{-3}	0.47, −0.22	0.443, −0.261	0.814, −0.734

$^aR_1 = [\sum||F_o| - |F_c||]/[\sum|F_o|]$ for $[F_o^2 > 2\sigma(F_o^2)]$, $wR_2 = \{[\sum w(F_o^2 - F_c^2)^2]/[\sum w(F_o^2)^2]\}^{1/2}$ [all data].

dx.doi.org/10.1021/ic301777y | *Inorg. Chem.* 2012, 51, 11155−11167

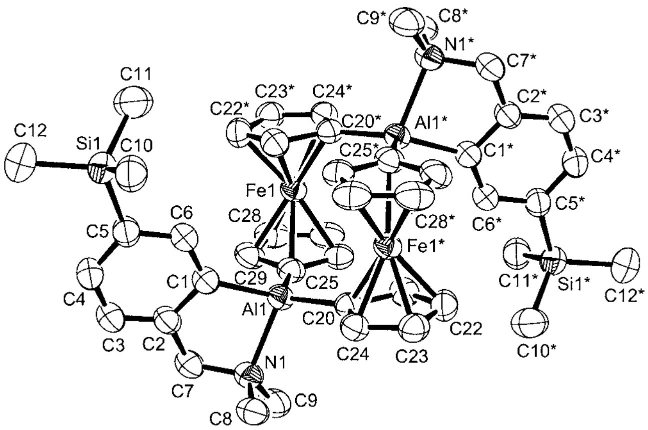

Figure 2. Molecular structure of **4a** with thermal ellipsoids at the 50% probability level. Hydrogen atoms are omitted for clarity. For a thermal ellipsoid plot of **4b** see Supporting Information, Figure S1. Selected atom−atom distances [Å] and bond angles [deg] for **4a**: Al1−N1 = 2.071(2), Al1−C1 = 1.985(3), Al1−C20 = 1.964(3), Al1−C25 = 1.972(3), Fe1···Fe1* = 5.3946(8), C1−Al1−C20 = 122.84(11), C1−Al1−C25 = 114.47(12), C1−Al1−N1 = 84.96(10), N1−Al1−C20 = 107.62(10), N1−Al1−C25 = 102.67(10), C20−Al1−C25 = 116.21(11). Selected atom−atom distances [Å] and bond angles [deg] for **4b**: Ga1−N1 = 2.173(2), Ga1−C1 = 1.976(3), Ga1−C20 = 1.968(3), Ga1−C25 = 1.963(3), Fe1···Fe1* = 5.4277(8), C1−Ga1−C20 = 114.60(12), C1−Ga1−C25 = 123.15(11), C1−Ga1−N1 = 83.35(10), N1−Ga1−C20 = 101.47(10), N1−Ga1−C25 = 106.25(10), C20−Ga1−C25 = 117.65(12). Symmetry transformation used to generate equivalent atoms (*): $-x + 1$, $-y$, $-z$.

arenophanes before;[23] however, compounds **4a** and **4b** turned out to be sparingly soluble in common organic solvents. A ^{13}C NMR spectrum of **4b** employing $CDCl_3$ could be measured. In contrast, the instability of the aluminum species **4a** in $CDCl_3$ and its poor solubility in other deuterated solvents prevented its ^{13}C NMR analysis.

Similar to the reaction shown in Scheme 2, the reactivity of the two halides **3a** and **3b** (Scheme 1) toward Li_2fc was explored. ^{1}H NMR analysis of crude products revealed the presence of the targeted [1.1]FCPs by typical signal patterns in the Cp region [(Mpysm)Al-bridged [1.1]FCP: δ 4.17, 4.49, 4.69, and 5.31 (C_6D_6); (Mpysm)Ga-bridged [1.1]FCP: δ 4.18, 4.41, 4.64, and 5.17 (C_6D_6)]. In addition to these sharp peaks, reaction mixtures always exhibited broad signals indicating the presence of oligomeric ferrocenylalumanes and gallanes, respectively.[22b] Despite our best efforts, we were not able to isolate the [1.1]FCPs from these mixtures.

Synthesis of Bis(ferrocenyl) Species with Aluminum, Gallium, and Silicon as Bridging Elements. One of the motivations to prepare [1.1]FCPs was to investigate the interaction between both redox-active iron atoms. In [1.1]FCPs, the relative orientation of ferrocene moieties is fixed. To address the question if the degree of interaction between two ferrocene moieties depends on their orientation, related compounds exhibiting a higher flexibility were targeted. Therefore, bis(ferrocenyl) species of aluminum and gallium were prepared (Scheme 3), which were equipped with the same intramolecularly coordinating ligands employed for the synthesis of [1.1]FCPs. Furthermore, we wanted to find out, if the type of bridging element had a significant influence on the metal−metal interaction and, thus, prepared bis(ferrocenyl)-silanes ($\mathbf{7^{Me}}$, $\mathbf{7^{Et}}$; Scheme 3) were prepared. Whereas the isolated yields for the group-13-containing species were only low to moderate (21−47%), those of the silanes were expectedly better ($\mathbf{7^{Me}}$: 70%; $\mathbf{7^{Et}}$: 72%). The synthesis of the silane $\mathbf{7^{Me}}$ had been described in a patent before,[28] where LiFc was prepared in situ from ClHgFc and *n*BuLi; we prepared LiFc from FcH and *t*BuLi in thf as described in the literature.[29] Furthermore, Manners et al. found small amounts of $\mathbf{7^{Me}}$ in mixtures of oligomers of various chain lengths obtained by anionic ROP of dimethylsila[1]ferrocenophane.[30]

Scheme 3. Synthesis of Bis(ferrocenyl) Species

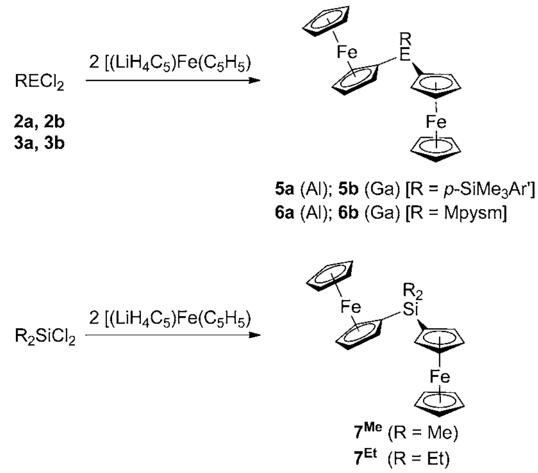

All bis(ferrocenyl) species have been characterized by NMR spectroscopy, mass spectrometry, and elemental analysis. Furthermore, the molecular structures of the aluminum atom species **6a** and the two silanes $\mathbf{7^{Me}}$ and $\mathbf{7^{Et}}$ were solved by single-crystal X-ray analyses (Figure 3 and 4; Table 2).[31] All four aluminum- and gallium-containing bis(ferrocenyl) com-

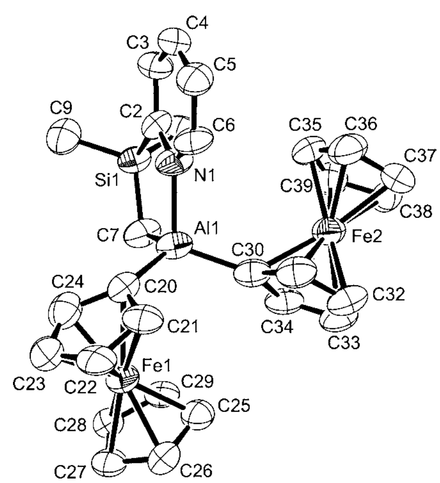

Figure 3. Molecular structure of **6a** with thermal ellipsoids at the 50% probability level. Hydrogen atoms are omitted for clarity. Selected atom−atom distances [Å] and bond angles [deg] for **6a** (values in braces refer to the second independent molecule that is not shown): Al1−N1 = 2.000(7) {2.034(7)}, Al1−C7 = 1.977(8) {1.980(7)}, Al1−C20 = 1.962(9) {1.962(9)}, Al1−C30 = 1.930(9) {1.950(8)}, Al1···Fe1 = 3.416(3) {3.403(3)}, Al1···Fe2 = 3.667(3) {3.680(3)}, Fe1···Fe2 = 6.045(2) {6.125(2)}, C7−Al1−C20 = 115.3(4) {114.8(3)}, C7−Al1−C30 = 117.1(3) {118.4(3)}, C7−Al1−N1 = 96.1(3) {94.8(3)}, N1−Al1−C20 = 106.8(3) {106.4(3)}, N1−Al1−C30 = 108.1(3) {108.4(3)}, C20−Al1−C30 = 111.5(3) {111.7(3)}, Al1−C20−Centr$^{C20-C24}$ = 166.7(5) {168.1(5)}, Al1−C30−Centr$^{C30-C34}$ = 177.2(6) {176.3(6)}.

dx.doi.org/10.1021/ic301777y | *Inorg. Chem.* 2012, 51, 11155−11167

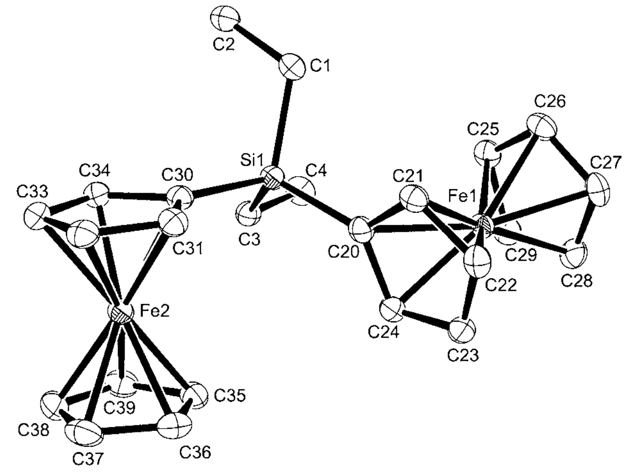

Figure 4. Molecular structure of 7^{Et} with thermal ellipsoids at the 50% probability level. Hydrogen atoms are omitted for clarity. For a thermal ellipsoid plot of 7^{Me} see Supporting Information, Figure S2. Selected atom−atom distances [Å] and bond angles [deg] for 7^{Et} (respective values of 7^{Me} given in braces): Si1−C1 = 1.880(2) {1.8677(17)}, Si1−C3 = 1.876(2) {1.8646(17)}, Si1−C20 = 1.861(2) {1.8580(16)}, Si1−C30 = 1.866(2) {1.8681(16)}, Si1···Fe1 = 3.5765(7) {3.4804(5)}, Si1···Fe2 = 3.5162(7) {3.5412(5)}, Fe1···Fe2 = 6.1409(6) {6.3150(4)}, C1−Si1−C3 = 111.23(10) {109.23(8)}, C1−Si1−C20 = 108.51(10) {109.10(8)}, C1−Si1−C30 = 108.49(9) {108.49(7)}, C3−Si1−C20 = 114.47(10) {112.17(7)}, C3−Si1−C30 = 106.47(9) {111.91(7)}, C20−Si1−C30 = 107.44(9) {105.81(7)}. Si1−C20−Centr$^{C20-C24}$ = 176.31(15) {177.78(12)}, Si1−C30−Centr$^{C30-C34}$ = 178.57(17) {177.88(12)}.

Table 2. Crystal and Structural Refinement Data for Compounds 6a, 7^{Me}, and 7^{Et}

	6a	7^{Me}	7^{Et}
empirical formula	$C_{28}H_{30}AlFe_2NSi$	$C_{22}H_{24}Fe_2Si$	$C_{24}H_{28}Fe_2Si$
fw	547.30	428.20	456.25
cryst. size/mm^3	0.21 × 0.21 × 0.01	0.32 × 0.14 × 0.06	0.30 × 0.24 × 0.06
cryst. system, space group	triclinic, $P\bar{1}$	monoclinic, $P2_1/n$	triclinic, $P\bar{1}$
Z	4	4	2
a/Å	10.6268(9)	8.0197(3)	7.4304(4)
b/Å	12.8724(10)	22.8843(6)	10.6917(5)
c/Å	18.6478(17)	10.1397(4)	13.0227(6)
α/deg	88.174(7)	90	80.412(4)
β/deg	82.917(7)	90.662(3)	81.259(4)
γ/deg	87.039(7)	90	86.783(4)
volume/Å^3	2527.2(4)	1860.77(11)	1007.77(9)
ρ_{calc}/mg m^{-3}	1.438	1.529	1.504
temperature/K	100	100	100
μ_{calc}./ mm^{-1}	1.25	1.63	1.51
θ range/deg	1.6−25.0	1.8−25.0	1.6−25.0
reflns collected/unique	13945/6615	17039/3277	10498/3546
absorption correction	multiscan	multiscan	multiscan
data/restraints/params	6615/94/599	3277/0/228	3546/0/246
goodness-of-fit	0.581	1.036	0.880
R_1 [$I > 2\sigma(I)$]^a	0.0421	0.0202	0.0255
wR_2 (all data)^a	0.0886	0.0495	0.0576
largest diff. peak and hole, $\Delta\rho_{elect}$/e Å^{-3}	0.28, −0.23	0.33, −0.24	0.41, −0.35

$^a R_1 = [\sum||F_o| - |F_c||]/[\sum|F_o|]$ for $[F_o^2 > 2\sigma(F_o^2)]$, $wR_2 = \{[\sum w(F_o^2 - F_c^2)^2]/[\sum w(F_o^2)^2]\}^{1/2}$ [all data].

pounds (**5a**, **5b**, **6a**, **6b**) show pattern in ^{1}H and ^{13}C NMR spectra consistent with time-averaged C_s symmetrical molecules. Recently, we characterized species (Mamx)EFc$_2$ [E = Al (**8a**), Ga (**8b**)] to better understand the structure and properties of respective poly(ferrocene)s equipped with the same bridging units.[22a] Similar to the species of type **5** and **6**, compounds **8a** and **8b** exhibit a plane of symmetry in solution, which can be explained with fast rotations of both Fc moieties. Expectedly, the Fc groups in the two silanes 7^{Me} and 7^{Et} also rotate fast, so that signal patterns in NMR spectra can be interpreted by assuming C_{2v} symmetrical species on time average. As mentioned before, species 7^{Me} was isolated before and our NMR data matches those reported.[30]

Figure 3 depicts the molecular structure of one of the two crystallographically independent molecules of **6a**. The covalent bonds around the aluminum have a similar length as those of the aluminum-bridged [1.1]FCP **4a** (Figure 2). The most interesting aspect of the molecular structure of **6a** is the different degree of bending of the two Fc moieties toward aluminum. Such a bending has been described for boryl-substituted ferrocenes (FcBX$_2$) and was expressed with a dip angle α^* (Figure 5).[32,33] In species **6a**, the Fc moiety (Fe2)

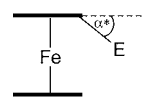

Figure 5. Definition of the dip angle $\alpha^* = 180 - \alpha(\text{Cp}^{centr}-\text{C}^{ipso}-\text{E})$[32].

close to the pyridyl group exhibits dip angles α^* of only 2.8(6) and 3.7(6)°, respectively, whereas the other Fc moiety (Fe1) exhibits dip angles α^* of 13.3(5) and 11.9(5)°, respectively (Figure 3). For borylferrocenes, α^* decreases with decreasing Lewis acidity of the boryl group. Within this series, Br$_2$BFc showed the largest experimentally determined α^* angles of 17.7 and 18.9° for two crystallographically independent molecules.[32,34] The dip angles of 11.9(5) and 13.3(5)° found for **6a** are comparable to those determined for Me$_2$BFc (α^* = 13.0°) and (HO)MeBFc (α^* = 10.3, 10.8, and 12.9°).[32] Recently, the silicon cation *t*BuMeSiFc$^+$ was characterized crystallographically, showing an extreme dip angle of 44.8°,[35] which is significantly larger than that of the well-known species Ph$_2$CFc$^+$ (α^* = 20.7°).[36] For the known systems, it has been shown that the bending is caused by a direct bonding interaction between the Lewis-acid atom and iron.[32,37] For the strongly bent silicon moiety in *t*BuMeSiFc$^+$, a 3c-2e bond between silicon, iron, and one of the carbon atoms of the unsubstituted Cp ring was discussed.[35]

As expected, molecular structures of both bis(ferrocenyl)-silanes 7^{Me} and 7^{Et} are very similar (Figure 4). Silicon atoms like those in 7^{Me} and 7^{Et} should not exhibit any significant Lewis acidity and bending toward the Fc moieties is not expected, an expectation that is confirmed by measured α^* angles of only 2.12(12) and 2.22(12)° for 7^{Me}, and 1.43(17) and −3.69(15)° for 7^{Et}.

Electrochemistry. The redox behavior of the [1.1]FCPs **4** and the bis(ferrocenyl) species **5**, **6**, **7**, and **8** were investigated with cyclic voltammetry using CH$_2$Cl$_2$ and tetrahydrofuran (thf), respectively, as solvents and [*n*Bu$_4$N][PF$_6$] as the electrolyte (Table 3).[38] While all gallium and silicon compounds gave meaningful and interpretable data (Table 3), all aluminum compounds were problematic with the exception of **8a**. The cyclic voltammograms (CVs) for [1.1]FCPs should

Table 3. Measured Formal Potentials versus FcH/FcH⁺ [V] of [1.1]FCPs and Bis(ferrocenyl) Species[a]

	$E°'$	$E°'$	$\Delta E°'$	Fe···Fe/Å[b]
4b (CH_2Cl_2)	−0.049	0.260	0.309	5.4277(8)[c]
4b (thf)	−0.091	0.127	0.218	
5b (CH_2Cl_2)	−0.002	0.136	0.138	
5b (thf)	0.224		0	
6b (CH_2Cl_2)	0.117	0.256	0.139	
6b (thf)	0.066		0	
$7^{Me}/7^{Et}$ (CH_2Cl_2)	0.071/0.128	0.257/0.332	0.186/0.204	6.3150(4)/6.1409(6)[c]
$7^{Me}/7^{Et}$ (thf)	0.176/0.191		0/0	
8a (CH_2Cl_2)	−0.032	0.135	0.167	5.6833(7)[d]
8a (thf)	0.079		0	
8b (CH_2Cl_2)	0.044	0.201	0.157	5.5944(9)[d]
8b (thf)	0.200		0	

[a]0.1 M [nBu$_4$N][PF$_6$]; scan rate of 50 mV/s. [b]Values from single-crystal X-ray structure determinations; see text for discussion. [c]This work. [d]Taken from ref 22a.

provide two, distinct redox couples, whose formal potential separation is dictated by the extent to which the presence of a charge on one ferrocene perturbs the redox potential of the neighboring center. Furthermore, assuming that (1) the diffusion coefficients for the three redox forms (the neutral molecule, the monovalent cation, and the divalent cation) of the [1.1]FCPs are not significantly different, (2) each redox couple has a transfer coefficient close to 0.5, and (3) each redox event corresponds to a single-electron transfer reaction, then it is expected that each individual redox event should provide identical peak currents when isolated from all other current contributions.[39] The gallium-bridged species **4b** showed precisely this behavior with two redox events ($\Delta E°'$ = 0.309 V) and corrected peak heights that are essentially identical in magnitude. A cursory inspection of the CV for the aluminum compound **4a** (Figure 6a) seems comparable as two main redox events are clearly evident. However, a more detailed inspection reveals the presence of two small, additional, reduction waves (ca. −0.4 V and −0.6 V). The peak current of the second oxidation wave is also seen to be much larger than that of the first oxidation wave. Cumulatively, these features indicate poorer electrochemical stability of the aluminum compound and/or the presence of electroactive impurities in the samples. Nevertheless, if one interprets the four main peaks in the CV of **4a** as being caused by the ferrocene moieties of **4a**, then the splitting between the two formal potentials $\Delta E°'$ amounts to 0.332 V. This splitting is similar to that of the gallium compound **4b** ($\Delta E°'$ = 0.309 V), but its voltammetry needs to be taken with some caution for the reasons described above. As mentioned in the Introduction, the known aluminum-bridged [1.1]FCP **1a**, in contrast to its gallium counterpart **1b** (Chart 3), showed significantly different CVs (CH_2Cl_2/[nBu$_4$N]-[PF$_6$]).[8b] While the gallium species **1b** displayed the expected *two* one-electron redox events ($\Delta E°'$ = 0.30 V) the aluminum species **1a** displayed only *one* two-electron redox event.[8b] The published formal potential for the aluminum species at 0.36 V with respect to Ag/AgCl is where that of ferrocene is expected,[8b] indicating that a complete removal of the bridging moieties had taken place.[39] A reinvestigation of the CV of species **1a** in CH_2Cl_2 with [nBu$_4$N][PF$_6$] has shown that, in contrast to the published results, it displays two main redox event. However, as in the case of compound **4a**, the recorded CV peak heights were unequal. A CV of species **1a** was also recorded using the electrolyte [nBu$_4$N][B(C_6F_5)$_4$] with a weakly coordinating anion. However, again a highly asymmetrical CV was measured, now with an expected larger splitting between the main redox events (see Supporting Information, Figures S42 and S43).[40,41] The second pair of redox waves is right were the FcH/FcH⁺ appears and it is very likely that at least some of the increased current is due to the presence of ferrocene. Aluminum species, compared to respective gallium species, are much more sensitive, and we speculate that small amounts of fluoride ions or residual water from the electrolyte and solvent are causing degradation. In 2008, similar observations were made for the related [1.1]-chromarenophanes and [1.1]molybdarenophanes: only the gallium-bridged species gave reproducible results, while measurements of the aluminum species showed the presence of significant amounts of the parent bis(benzene) complexes.[23]

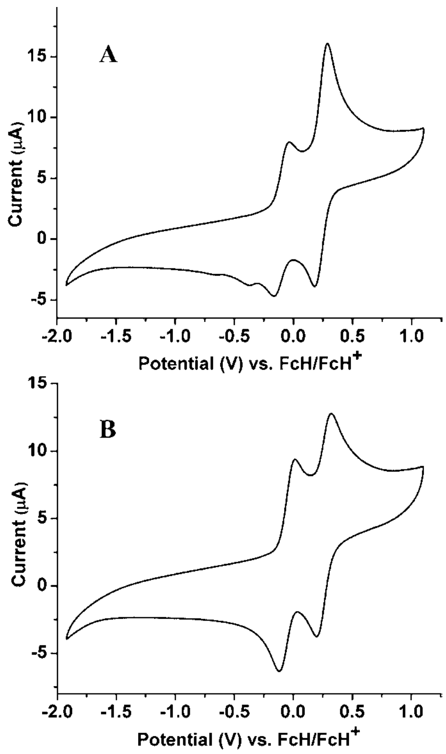

Figure 6. Cyclic voltammograms of **4a** (A) and **4b** (B) (CH_2Cl_2; 0.1 M [nBu$_4$N][PF$_6$]; scan rate = 50 mV/s).

As shown in Table 3, the measured $\Delta E°'$ values for the bis(ferrocenyl) species were found in the range 0.138−0.167 V

dx.doi.org/10.1021/ic301777y | Inorg. Chem. 2012, 51, 11155−11167

and are significantly smaller compared to those of the [1.1]FCPs **4a** and **4b**. The largest splitting was found for the aluminum compound **8a** ($\Delta E^{\circ\prime}$ = 0.167 V), which was the only aluminum species in this study that gave an expected CV (Figure 7). The CV of the respective gallium compound **8b** looks very similar with a slightly smaller $\Delta E^{\circ\prime}$ value of 0.157 V (Figure 7).

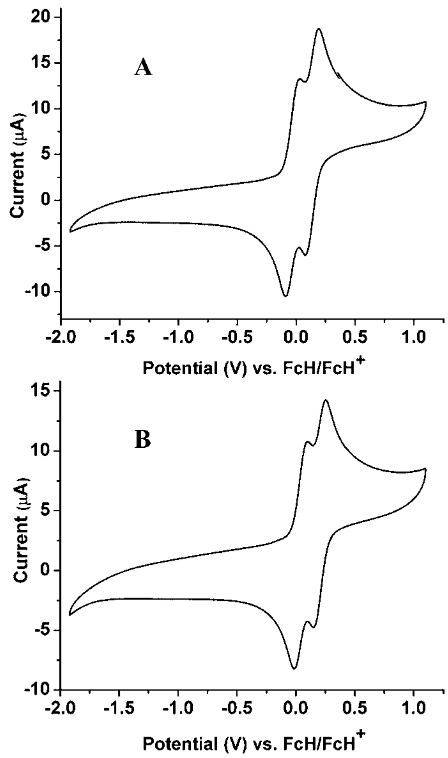

Figure 7. Cyclic voltammograms of **8a** (A) and **8b** (B) (CH_2Cl_2; 0.1 M [nBu$_4$N][PF$_6$]; scan rate = 50 mV/s).

Geiger et al. systematically investigated the medium effect on the splitting $\Delta E^{\circ\prime}$ and have shown that for electrochemically generated cations, solvents of low polarity and low donor number (DN)[42] cause the largest values of $\Delta E^{\circ\prime}$.[40,41] To test if the solvent effect[43] also holds true for the compounds described here, CH_2Cl_2 and thf solutions were investigated for all species. Furthermore, as aluminum species can be sensitive toward chlorinated solvents, we wanted to find out if thf improves the appearance of their CVs; however, this was not the case. As expected, all $\Delta E^{\circ\prime}$ values were significantly reduced by changing from CH_2Cl_2 (DN = 0) to thf (DN = 20) (Table 3).[40,41] Whereas the [1.1]FCP **4b** still showed resolved waves, all other species listed in Table 3 displayed only one redox wave. The $\Delta E^{\circ\prime}$ value of the [1.1]FCP **4b** diminished from 0.309 V (CH_2Cl_2) to 0.218 V (thf). As the splitting between formal potentials of the bis(ferrocenyl) species is already small in CH_2Cl_2, it is not surprising that it is absent in thf solutions.[44]

As mentioned above, the only aluminum species that exhibited the expected two, one-electron oxidations in the CV was compound **8a** (Figure 7). The overall shape of its CV is very similar to that of the gallium compound **8b** (Figure 7). While the aluminum compound **8a** gets oxidized at lower potentials compared to its gallium analogue **8b**, their $\Delta E^{\circ\prime}$ values are very similar (**8a**: 0.167 V; **8b**: 0.157 V; Table 3). Aluminum is significantly less electronegative compared to gallium, resulting in an increase of the electron density on the ferrocenyl moieties, explaining the increased ease by which **8a** gets oxidized compared to **8b** [Allred–Rochow electronegativities:[45] 1.47 (Al), 1.82 (Ga)].

Why is compound **8a** the only electrochemically well-behaved aluminum species in our study? All the aluminum and gallium compounds were equipped with intramolecularly coordinating ligands (Chart 2). The Mamx ligand stands out as the only ligand used that carries a bulky group in the vicinity of the group 13 element. This *ortho*-*t*Bu group is directed toward the fifth coordination site on the group 13 element and, hence, provides steric protection. For example, in contrast to the bis(ferrocenyl) species **6a** (Figure 3), the ferrocenyl units of species **8a** and **8b** are not bent *toward* the group 13 element, but *away* from it (e.g., **8a**: α^* = −9.11°).[22a] One can assume that the fifth coordination site of the group 13 elements is of key importance for any substitution reaction, including hydrolysis, as a Lewis acid–base adduct will likely form first. We speculate that this extra protection provided by the *ortho*-*t*Bu group of the Mamx ligand efficiently suppresses any unwanted reactions during the electrochemical measurement.

Recently, a comprehensive study on the electronic coupling in bis(ferrocene) species of the type ($Cp^*FeC_5H_4)ER_2$ with bridging moieties ER_2 of CMe_2, $SiMe_2$, and $GeMe_2$ was undertaken.[46] From the analysis of the intervalence charge-transfer band of the mixed-valence monocations ($Cp^*FeC_5H_4$)-ER_2^+ it was revealed that the coupling decreases in the order of C > Si > Ge. The $\Delta E^{\circ\prime}$ values (thf/[nBu$_4$N][PF$_6$]), determined by square-wave voltammetry, showed the same trend [0.113 (C), 0.093 (Si), and 0.073 (Ge) V], which is consistent with Fe···Fe distances. The authors concluded that an electrostatic through-space and not a through-bond mechanism was operative.[46] As mentioned before, species $\mathbf{7}^{\mathbf{Me}}$ is a known species[28,30] and was investigated with electrochemical methods before.[47,30] The published $\Delta E^{\circ\prime}$ value of 0.15 V was determined using a 1:1 solvent mixture of CH_2Cl_2 and MeCN and [nBu$_4$N][PF$_6$] as the electrolyte.[30] Our value for $\mathbf{7}^{\mathbf{Me}}$ in CH_2Cl_2 is with 0.186 V (Table 3) expectedly higher. We also determined the CV of $\mathbf{7}^{\mathbf{Me}}$ in MeCN (Supporting Information, Figure S35) and found a splitting value $\Delta E^{\circ\prime}$ of 0.142 V, nearly identical to the published value of 0.15 V in CH_2Cl_2/MeCN. The $\Delta E^{\circ\prime}$ values of $\mathbf{7}^{\mathbf{Me}}$ and $\mathbf{7}^{\mathbf{Et}}$ are with 0.186 and 0.204 V (Table 3), respectively, similar and slightly larger than those measured for the gallium species **5b**, **6b**, and **8b** ($\Delta E^{\circ\prime}$ = 0.138–0.159 V) and of the aluminum species **8a** ($\Delta E^{\circ\prime}$ = 0.167 V). Table 3 also lists the Fe···Fe distances known from single-crystal X-ray analysis. For the silicon species, exhibiting the largest $\Delta E^{\circ\prime}$ values, the Fe···Fe distances are significantly larger [$\mathbf{7}^{\mathbf{Me}}$: 6.3150(4) Å; $\mathbf{7}^{\mathbf{Et}}$: 6.1409(6) Å] than those found for the Mamx-containing aluminum and gallium species [**8a**: 5.6833(7) Å; **8b**: 5.5944(9) Å]. The only other bis(ferrocenyl) species for which the molecular structure could be determined in the solid state was the aluminum compound **6a** (Figure 3) and Fe···Fe distances of 6.045(2) and 6.125(2) Å for two independent molecules were found. The covalent radii of Al and Ga are nearly identical and one can assume that the Fe···Fe distance in **6b** is very similar to those determined for **6a**. The gallium compound **6b** showed with 0.139 V one of the smallest $\Delta E^{\circ\prime}$ values (Table 3). Of course, the Fe···Fe distances discussed so far are not necessarily identical to those present in solution. As evident from NMR spectra of all bis(ferrocenyl) species, both Fc units rotate fast, and one could imagine that Fe···Fe distances vary depending on the relative orientation of the two Fc moieties. For the Mamx-containing species, two different conformers were found in the solid state (Chart 4). While the

Chart 4. Two Conformers of (Mamx)EFc$_2$ [E = Al (8a), Ga (8b)][22a]

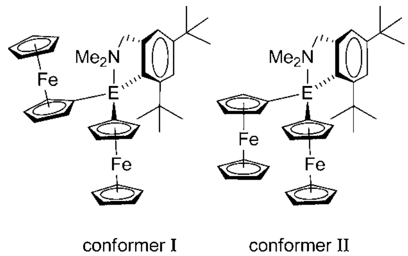

aluminum species **8a** showed the Fc moieties pointing in opposite directions (conformer I), those of the gallium species **8b** were approximately parallel to each other (conformer II).[22a] However, the Fe···Fe distances in both species were very similar [**8a**: 5.6833(7) Å; **8b**: 5.5944(9) Å], which indicates that rotations of Fc moieties do not alter the Fe···Fe distances significantly. Overall, there is no obvious correlation between the Fe···Fe distances and $\Delta E^{\circ\prime}$ values of the bis(ferrocenyl) species equipped with different bridging moieties (Table 3).

The $\Delta E^{\circ\prime}$ values of the [1.1]FCP **4b** and the bis(ferrocenyl) compound **5b**, both equipped with the same bridging moiety, are significantly different (**4b**: 0.309 V; **5b**: 0.138 V). While the Fe···Fe distance in **4b** could be determined that of species **5b** is unknown. However, the Fe···Fe distance of the closely related compound **8b** was found to be 5.5944(9) Å (Table 3),[22a] which is very similar to 5.4277(8) Å measured for the [1.1]FCP **4b** (Figure 2; Table 3). Obviously, the huge difference in $\Delta E^{\circ\prime}$ values cannot be rationalized on the basis of Fe···Fe distances. As pointed out earlier, the relative orientations of the two fc units of [1.1]FCPs (e.g., **4b**) are fixed, while the Fc moieties of bis(ferrocenyl) compounds (e.g., **5b**) can freely rotate. We speculate that the flexibility in bis(ferrocenyl) compounds allows for an effective solvation of both Fc moieties, resulting in an effective screening of positive charges. In contrast, the solvation of [1.1]FCPs will be less effective as a solvent penetration between both fc moieties will be hindered; hence, the electrostatic interaction between the two iron centers in the monocations will be stronger than in bis(ferrocenyl) compounds, giving larger $\Delta E^{\circ\prime}$ values. In addition, in conformer I of bis(ferrocenyl) compounds (Chart 4) one Cp moiety is in between the two Fe atoms, a scenario that is not possible for [1.1]FCPs. It is feasible that this extra electron density provided by the Cp ligand also contributes to the screening of charges.

■ SUMMARY AND CONCLUSION

The two new [1.1]FCPs **4a** (Al) and **4b** (Ga) were prepared and crystallized as *anti* isomers. As expected, their structures are very similar to the known [1.1]FCPs (**1a**, **1b**; Chart 3). Ferrocenyl-substituted aluminum and gallium compounds are rare.[48] The new bis(ferrocenyl) compounds of aluminum (**5a**, **6a**) and gallium (**5b**, **6b**) equipped with two different ligands capable of intramolecular donation were prepared. Only the aluminum compound **6a** gave crystals of sufficient quality that allowed a structure determination by X-ray crystallography (Figure 3). One of the two Fc units in species **6a** is significantly bent toward the open coordination site of aluminum [dip angle α^* = 13.3(5) and 11.9(5)°]. Such an effect is well-known for boron compounds and other species with Lewis-acidic moieties in this *pseudo* benzylic position, but had never been observed for aluminum compounds. The bending of a Fc unit in **6a** illustrates that the aluminum atom still possess Lewis-acidity despite being 4-fold coordinated.

The bis(ferrocenyl) species **5a**, **5b**, **6a**, and **6b** were prepared so that Fe–Fe interactions could be investigated and compared with those in the related [1.1]FCPs **4a** and **4b**. The series of CV measurements also included the recently published bis(ferrocenyl) compounds (Mamx)EFc$_2$ [**8a** (Al), **8b** (Ga)] and the known aluminum-bridged [1.1]FCP **1a** (Chart 3). To include bis(ferrocenyl) species with saturated bridging moieties, the silanes R_2SiFc_2 [R = Me (7^{Me}), Et (7^{Et})] were prepared, and their CVs were determined. While all gallium and silicon compounds gave meaningful and interpretable data (Table 3), all aluminum compounds were problematic with the exception of **8a** (Chart 4, Figure 7). The fact that **8a** was the only well-behaved aluminum species is probably due to the steric protection of the Lewis-acidic aluminum atom by the bulky Mamx ligand, which suppresses unwanted degradation reactions. The degree of splitting between formal potentials of bis(ferrocenyl) compounds **5b**, **6b**, 7^{Me}, 7^{Et}, **8a**, and **8b** varied between 0.138–0.204 V ($\Delta E^{\circ\prime}$ in CH_2Cl_2; Table 3).

Recently, it had been shown that for group-14-bridged bis(ferrocenyl) compounds a through-space coupling is operative and, hence, through-bond coupling is relatively unimportant.[46] In this study, a qualitative correlation between $\Delta E^{\circ\prime}$ values and Fe···Fe distances was found: the larger the distances, the smaller the $\Delta E^{\circ\prime}$ values. Our $\Delta E^{\circ\prime}$ values measured for the two silanes 7^{Me} and 7^{Et} seem to support such a correlation, if Fe···Fe distances found in the solid state are indicative of Fe···Fe distances in solution: species 7^{Et} with the *smaller* Fe···Fe distance gave the *stronger* interaction (Table 3). Structural evidence suggests that Fe···Fe distances in bis(ferrocenyl) aluminum and gallium species are *shorter* than in the silicon compounds 7^{Me} and 7^{Et}, but their $\Delta E^{\circ\prime}$ values are *smaller*. Geiger et al. performed a comprehensive study of solvent and electrolyte effects on $\Delta E^{\circ\prime}$ values by keeping the analyte constant.[40,41] For electrochemically produced cations, $\Delta E^{\circ\prime}$ can be maximized by applying solvents of low polarity and low donor number and a weakly ion-pairing electrolyte anion. We investigated a series of different species under the same conditions, where all the electrochemically produced cations were different. Therefore, for all cations the overall effects of ion pairing and solvation must be different. All the seemingly similar bis(ferrocenyl) compounds are, with respect to all the factors that govern the splitting between formal potentials, too different, and a correlation of $\Delta E^{\circ\prime}$ with Fe···Fe distances cannot be expected.

The splitting between formal potentials in [1.1]FCPs is significantly larger than in related ferrocenyl compounds, even though the Fe···Fe distances are similar [e.g., $\Delta E^{\circ\prime}$ = 0.309 (**4b**), 0.138 (**5b**) V]. It might be that the flexibility in bis(ferrocenyl) compounds allows for an effective solvation of both Fc moieties, resulting in an effective screening of positive charges leading to a small $\Delta E^{\circ\prime}$. However, in the absence of additional data, the latter statement remains speculative.

■ EXPERIMENTAL SECTION

Syntheses. All syntheses were carried out using standard Schlenk and glovebox techniques. Solvents were dried using an MBraun Solvent Purification System and stored under nitrogen over 3 Å molecular sieves. All solvents for NMR spectroscopy were degassed prior to use and stored under nitrogen over 3 Å molecular sieves. ^{1}H and ^{13}C NMR spectra were recorded on a 500 MHz Bruker Avance NMR spectrometer at 25 °C in C_6D_6 and $CDCl_3$, respectively. ^{1}H chemical shifts were referenced to the residual protons of the deuterated solvents (δ 7.15 for C_6D_6 and 7.26 for $CDCl_3$); ^{13}C chemical shifts were referenced to the C_6D_6 signal at δ 128.00 and $CDCl_3$ signal at δ 77.00. Mass spectra were measured on a VG 70SE and were reported in the form m/z (rel intens) [M^+] where "m/z" is the mass observed, "rel intens" is the intensity of the peak relative to the most intense peak and "M^+" is the molecular ion or fragment; only characteristic mass peaks are reported. For isotopic pattern, only the mass peak of the isotopoloque or isotope with the highest natural abundance is listed. Elemental analyses were performed on a Perkin-Elmer 2400 CHN Elemental Analyzer using V_2O_5 to promote complete combustion.

Note that small amounts of ferrocene ($FeCp_2$) were present in the isolated products **4a**, **4b**, **5a**, **5b**, **6a**, and **6b**; complete removal of this impurity was not successful. The three aluminum species show larger amounts of ferrocene impurities compared to their gallium counterparts (see NMR spectra in the Supporting Information). The difficulties to obtain analytically pure aluminum species reflect their higher sensitivity toward hydrolysis compared to respective gallium compounds. Elemental analysis gave carbon values for **4a**, **5a**, and **6a** below their calculated amounts. All three compounds have calculated amounts of C above 60%, and carbide formation might have contributed to the lower than expected C values. All new compounds showed molecular ions of fitting masses in high-resolution mass spectrometry.

Reagents. The compounds $(LiC_5H_4)Fe(C_5H_5)$ (LiFc),[29] $(LiC_5H_4)_2Fe\cdot 2/3$tmeda ($Li_2fc\cdot 2/3$tmeda),,[49] 2-(trimethylsilyl)-pyridine,[50] and **2b**[19a] were synthesized according to literature procedures. The known species 1-bromo-4-[(dimethylamino)methyl]-benzene[51] and 1-[(dimethylamino)methyl]-4-trimethylsilylbenzene[52] were synthesized according to the published procedures with small alterations (see Supporting Information). $AlCl_3$ (98%), ferrocene (98%), *n*BuLi (2.8 M in hexanes), *t*BuLi (1.7 M in pentane), Me_3SiCl (98%), and C_6D_6 (99.6 atom % D) were purchased from Sigma Aldrich; $AlCl_3$ was sublimed prior to use. $GaCl_3$ (Alfa Aesar; 99.999%), 2-bromopyridine (Alfa Aesar; 99%), and 1-bromo-4-(bromomethyl)-benzene (Alfa Aesar; 99%) were purchased from VWR. *N,N,N′,N′*-tetramethylethylenediamine (tmeda) (Acros Organics; 99%) was purchased from Fisher Scientific.

Electrochemical Measurements. A computer controlled system, consisting of a HEKA potentiostat PG590 (HEKA, Mahone Bay, NS, Canada) was used for the cyclic voltammetry experiments. Data was collected using a multifunction DAQ card (PCI 6251 M Series, National Instruments Austin, Texas) and in-house software written in the LabVIEW environment. Glassy carbon (BAS, 3 mm) was used as the working electrode. The quasi-reference electrode (QRE) was a silver wire and all measurements were made against the QRE. A coiled gold wire was used as the auxiliary electrode. Before each measurement, 1 mM solutions of samples were freshly prepared in dry organic solvents with 0.1 M [nBu$_4$N][PF$_6$] as the supporting electrolyte. The electrolyte was dried overnight under high vacuum at 100 °C before. The scan rate for the CVs reported was 50 mV/s. The measurements were conducted inside a glovebox and taken at ambient temperature.

Synthesis of Dichloro{2-[(dimethylamino)methyl]-5-(trimethylsilyl)phenyl-κ^2*C,N*}alumane (2a). *t*BuLi (1.7 M in pentane, 9.8 mL, 17 mmol) was added dropwise to a cold (0 °C) solution of 1-[(dimethylamino)methyl]-4-trimethylsilylbenzene (3.55 g, 15.1 mmol) in hexane (40 mL). The reaction mixture was warmed up to room temperature (r.t.) and stirred for 16 h, yielding a pale yellow solution with a white precipitate. The solid lithium salt was filtered off and dried under high vacuum (2.24 g, 10.5 mmol). Et_2O (30 mL) was added to the white solid, resulting a slurry which was cooled down to −78 °C. The cold slurry was added dropwise to a cold (−78 °C) solution of $AlCl_3$ (1.39 g, 10.4 mmol) in Et_2O (40 mL). The reaction mixture was warmed up to r.t. and stirred for 16 h, resulting in a pale yellow solution with a white precipitate. The solid was filtered off, and all volatiles were removed under high vacuum. Sublimation (110 °C, high vacuum) yielded analytically pure product **2a** as a colorless crystalline solid (2.33 g, 73%). ^{1}H NMR (C_6D_6): δ 0.26 (s, 9H, SiMe$_3$), 1.90 (s, 6H, NMe$_2$), 2.97 (s, 2H, CH$_2$), 6.75 (d, 1H, C$_6$H$_3$), 7.45 (d, 1H, C$_6$H$_3$), 7.91 (s, 1H, C$_6$H$_3$). ^{13}C NMR (C_6D_6): δ −1.09 (SiMe$_3$), 45.35 (CH$_2$), 64.72 (NMe$_2$), 125.06, 134.86, 140.64, 141.097 (C$_6$H$_3$). MS (70 eV) m/z (rel intens): 303 (15) [M^+], 288 (100) [M^+ − Me], 272 (16) [$C_{10}H_{13}AlCl_2NSi^+$], 245 (18) [$C_9H_{12}AlCl_2Si^+$]. HRMS (70 eV) m/z: calcd for $C_{12}H_{20}AlCl_2NSi$, 305.0528; found, 305.0521. Anal. Calcd for $C_{12}H_{20}AlCl_2NSi$ (304.27): C, 47.37; H, 6.63; N, 4.60. Found: C, 47.39; H, 6.55; N, 4.61.

Synthesis of Dichloro{[dimethyl(2-pyridyl)silyl]methyl-κ^2*C,N*}alumane (3a). *t*BuLi (1.7 M in pentane, 11.8 mL, 20.1 mmol) was added dropwise to a solution of 2-(trimethylsilyl)pyridine (2.89 g, 19.1 mmol) in Et_2O (30 mL) at −78 °C. After 40 min of stirring at −78 °C, a solution of $AlCl_3$ (2.44 g, 18.3 mmol) in Et_2O (30 mL) was added slowly at −78 °C. After the reaction mixture was stirred for 16 h at r.t., all volatiles were removed under vacuum. The product was dissolved in toluene (35 mL), and the precipitate was filtered off and washed with toluene (10 × 5 mL). All volatiles were removed at high vacuum at 90 °C and crystallization from toluene (5 mL) at ca. −25 °C yielded colorless crystals of **3a** (2.60 g, 47%). ^{1}H NMR (C_6D_6): δ −0.32 (s, 2H, CH$_2$), 0.02 (s, 6H, SiMe$_2$), 6.27 (m, 1H, Ar−H), 6.70 (m, 2H, Ar−H), 8.28 (m, 1H, Ar−H). ^{13}C NMR (C_6D_6): δ −0.60 (CH$_2$), 1.36 (SiMe$_2$), 124.92, 130.29, 139.35, 146.91, 171.05 (C$_5$H$_4$N). MS (70 eV) m/z (rel intens): 247 (7) [M^+], 232 (100) [M^+ − Me], 212 (11) [M^+ − Cl], 151 (11) [MH^+ − AlCl$_2$], 150 (15) [M^+ − AlCl$_2$], 106 (14) [$C_5H_4NSi^+$]. HRMS (70 eV) m/z: calcd for $C_8H_{12}Cl_2AlNSi$, 248.9902; found, 248.9901. Anal. Calcd for $C_8H_{12}AlCl_2NSi$ (248.16): C, 38.72; H, 4.87; N, 5.64. Found: C, 39.66; H, 5.32, N, 5.51.

Synthesis of Dichloro{[dimethyl(2-pyridyl)silyl]methyl-κ^2*C,N*}gallium (3b). *t*BuLi (1.7 M in pentane, 8.60 mL, 14.6 mmol) was added dropwise to a solution of 2-(trimethylsilyl)pyridine in Et_2O (25 mL) at −78 °C. After 40 min at −78 °C, the solution was slowly added to a solution of $GaCl_3$ (2.38 g, 13.5 mmol) in Et_2O (35 mL) at −78 °C. After the reaction mixture was stirred for 16 h at r.t., all volatiles were removed under vacuum. The crude product was dissolved in toluene (40 mL), and the precipitate was filtered off and washed with toluene (4 × 10 mL). Sublimation (120 °C; high vacuum) gave **3b** as a colorless, crystalline product (2.00 g, 50%) that contained only very minor impurities. Analytically pure product (1.36 g, 35%) was obtained by crystallization from toluene (4 mL). Crystals suitable for single-crystal X-ray analysis were obtained from toluene solution at −25 °C. ^{1}H NMR (C_6D_6): δ −0.07 (s, 2H, CH$_2$), −0.02 (s, 6H, SiMe$_2$), 6.42 (m, 1H, Ar−H), 6.77 (d, 1H, Ar−H), 6.82 (m, 1H, Ar−H), 8.41 (d, 1H, Ar−H). ^{13}C NMR (C_6D_6): δ −6.83 (CH$_2$), −1.11 (SiMe$_2$), 125.50, 130.28, 139.24, 146.80, 167.22 (C$_5$H$_4$N). MS (70 eV) m/z (rel intens): 291 (7) [M^+], 276 (100) [M^+ − Me], 256 (54) [M^+ − Cl], 170 (11) [(NC$_5$H$_4$)SiMeCH$_2$Cl$^+$], 149 (14) [$C_8H_7NSi^+$], 120 (16) [$C_6H_6NSi^+$], 106 (12) [$C_5H_4NSi^+$], 92 (11) [$C_5H_4Si^+$], 91 (15) [$C_5H_3Si^+$], 69 (14) [Ga]. HRMS (70 eV) m/z: calcd for $C_8H_{12}Cl_2GaNSi$, 290.9363; found, 290.9350. Anal. Calcd for $C_8H_{12}Cl_2GaNSi$ (290.90): C, 33.03; H, 4.16; N, 4.81. Found: C, 33.82; H, 4.33; N, 4.61.

Synthesis of Bis({2-[(dimethylamino)methyl]-5-(trimethylsilyl)phenyl-κ^2*C,N*}alumina)[1.1]ferrocenophane (4a). A solution of **2a** (0.710 g, 2.33 mmol) in Et_2O (30 mL) was added dropwise to a slurry of $(LiC_5H_4)_2Fe\cdot 2/3$tmeda (0.701 g, 2.55 mmol) in Et_2O (20 mL). The reaction mixture was stirred at r.t. for 16 h, resulting in a red solution with white precipitate. After the solid was filtered off, all volatiles were removed from the filtrate under vacuum. The resulting deep orange, sticky crude product was washed with hexane (3 × 50 mL), yielding the pure product **4a** as an orange solid (0.420 g, 43%). Crystals suitable for single-crystal X-ray analysis were obtained from thf solution at ca. −25 °C. Note: **4b** is poorly soluble in organic solvents, expect for chloroform. However, it slowly reacts with the solvent preventing its ^{13}C NMR analysis. ^{1}H NMR (C_6H_6): δ 0.43 (s, 18H, SiMe$_3$), 1.74 (s, 12H, NMe$_2$), 3.33 (s, 4H, CH$_2$), 4.01, 4.46, 4.60, 5.30 (pst, 8H, C_5H_4), 7.04 (d, 2H, C_6H_3), 7.64 (d, 2H, C_6H_3), 8.90 (s, 2H, C_6H_3). MS (70 eV) *m*/*z* (rel intens): 834 (12) [M^+], 206 (32) [$C_{12}H_{20}NSi^+$], 207 (45) [$C_{12}H_{21}NSi^+$], 186 (100) [$C_{10}H_{10}Fe^+$], 163 (11) [$C_{10}H_{15}Si^+$], 135 (14) [$C_9H_{13}N^+$], 134 (14) [$C_9H_{12}N^+$], 121 (29) [$C_5H_5Fe^+$]. HRMS (70 eV) *m*/*z*: calcd for $C_{44}H_{56}Fe_2Al_2N_2Si_2$, 834.2380; found, 834.2367. Anal. Calcd for $C_{44}H_{56}Al_2Fe_2N_2Si_2$ (834.75): C, 63.31; H, 6.76; N, 3.36. Found: C, 61.19; H, 7.00; N, 3.22.

Synthesis of Bis({2-[(dimethylamino)methyl]-5-(trimethylsilyl)phenyl-κ^2*C*,*N*}galla)[1.1]ferrocenophane (4b). A solution of **2b** (1.12 g, 3.23 mmol) in Et_2O (40 mL) was added dropwise to a slurry of $(LiC_5H_4)_2Fe\cdot 2/3$tmeda (0.998 g, 3.62 mmol) in Et_2O (30 mL). The reaction mixture was stirred at r.t. for 16 h, yielding a red solution with a white precipitate. After the solid was filtered off, all volatiles were removed from the filtrate under vacuum. The resulting deep orange, sticky crude product was washed with hexane (3 × 50 mL), yielding the pure product as an orange solid (0.701 g, 47%). Crystals suitable for single-crystal X-ray analysis were obtained from thf solution at −22 °C. ^{1}H NMR ($CDCl_3$): δ 0.40 (s, 18H, $SiMe_3$), 2.14 (s, 12H, NMe_2), 3.72 (s, 4H, CH_2), 3.86, 4.26, 4.32, 4.74 (pst, 8H, C_5H_4), 7.15 (d, 2H, C_6H_3), 7.50 (d, 2H, C_6H_3), 8.34 (s, 2H, C_6H_3). ^{1}H NMR (C_6D_6): δ 0.43 (s, 18H, $SiMe_3$), 1.84 (s, 12H, NMe_2), 3.28 (s, 4H, CH_2), 4.03, 4.40, 4.58, 5.22 (pst, 8H, C_5H_4), 7.07 (d, 2H, C_6H_3), 7.60 (d, 2H, C_6H_3), 8.80 (s, 2H, C_6H_3). ^{13}C NMR ($CDCl_3$): δ −0.72 ($SiMe_3$), 46.22 (NMe_2), 66.61 (CH_2), 70.02, 70.19, 70.52, 74.31, 74.81 (C_5H_4), 123.93, 131.97, 138.05, 142.00, 145.09, 149.54 (C_6H_3). MS (70 eV) *m*/*z* (rel intens): 920 (100) [M^+], 460 (19) [$C_{22}H_{29}FeGaNSi^+$], 69 (12) [Ga^+]. HRMS (70 eV) *m*/*z*: calcd for $C_{44}H_{56}Fe_2Ga_2N_2Si_2$, 920.1184; found, 920.1170. Anal. Calcd for $C_{44}H_{56}Fe_2Ga_2N_2Si_2$ (920.24): C, 57.43; H, 6.13; N, 3.04. Found: C, 56.94; H, 6.31; N, 2.91.

Synthesis of {2-[(Dimethylamino)methyl]-5-(trimethylsilyl)phenyl-κ^2*C*,*N*}bis(ferrocenyl)alumane (5a). A solution of **2a** (0.610 g, 2.00 mmol) in benzene (40 mL) was added dropwise to a slurry of LiFc (0.968 g, 5.04 mmol) in benzene (25 mL) at r.t. and stirred for 16 h, after which a red solution with an orange precipitate was obtained. After the solid was filtered off, all volatiles were removed under vacuum, yielding a red paste as the crude product. The product was extracted with cyclohexane (40 mL), the cyclohexane solution was concentrated to a volume of approximately 10 mL and kept at 6 °C for 16 h, resulting in orange crystals. The crystals were washed with hexane (2 × 5 mL) and dried under vacuum, yielding pure **5a** as an orange powder (0.568 g, 47%). ^{1}H NMR (C_6D_6): δ 0.35 (s, 9H, $SiMe_3$), 1.90 (s, 6H, NMe_2), 3.35 (s, 2H, CH_2), 4.02, 4.41, 4.45, 4.48 (pst, 8H, C_5H_4), 4.33 (s, 10H, C_5H_5), 7.01 (d, 1H, C_6H_3), 7.59 (d, 1H, C_6H_3), 8.50 (s, 1H, C_6H_3). ^{13}C NMR (C_6D_6): δ −0.73 ($SiMe_3$), 45.87 (NMe_2), 67.28 (CH_2), 68.12 (C_5H_5), 71.54, 71.65, 76.35, 77.21 (C_5H_4), 123.69, 132.87, 138.19, 142.96, 145.09 (C_6H_3). MS (70 eV) *m*/*z* (rel intens): 603 (100) [M^+], 301 (10) [$C_{17}H_{14}AlFe^+$], 186 (27) [$C_{10}H_{10}Fe^+$], 120 (10) [$C_5H_5Fe^+$]. HRMS (70 eV) *m*/*z*: calcd for $C_{32}H_{38}Fe_2AlNSi$, 603.1288; found, 603.1291. Anal. Calcd for $C_{32}H_{38}AlFe_2NSi$ (603.41): C, 63.70; H, 6.35; N, 2.32. Found: C, 60.02; H, 6.35; N, 2.11.

Synthesis of {2-[(Dimethylamino)methyl]-5-(trimethylsilyl)phenyl-κ^2*C*,*N*}bis(ferrocenyl)gallane (5b). A solution of **2b** (0.495 g, 1.43 mmol) in benzene (30 mL) was added dropwise to a slurry of LiFc (0.678 g, 3.53 mmol) in benzene (10 mL) at r.t. The resulting reaction mixture was stirred for 16 h, resulting in a red solution with an orange precipitate. After the solid was filtered off, all volatiles were removed under vacuum, yielding a red paste as the crude product. The product was extracted with cyclohexane (30 mL), the cyclohexane solution was concentrated to a volume of approximately 10 mL and kept at 6 °C for 16 h, resulting in orange crystals. The crystals were washed with hexane (2 × 5 mL) and dried under vacuum, yielding the product as an orange powder (0.568 g, 41%). ^{1}H NMR (C_6D_6): δ 0.35 (s, 9H, $SiMe_3$), 1.82 (s, 6H, NMe_2), 3.27 (s, 2H, CH_2), 4.01, 4.37, 4.44, 4.47 (pst, 8H, C_5H_4), 4.36 (s, 10H, C_5H_5), 7.04 (d, 1H, C_6H_3), 7.57 (d, 1H, C_6H_3), 8.46 (s, 1H, C_6H_3). ^{13}C NMR (C_6D_6): δ 0.68 ($SiMe_3$), 46.02 (NMe_2), 67.01 (CH_2), 68.18 (C_5H_5), 70.96, 71.08, 72.19, 75.50, 76.06 (C_5H_4), 124.24, 132.55, 138.59, 141.88, 144.54, 150.22 (C_6H_3). MS (70 eV) *m*/*z* (rel intens): 645 (75) [M^+], 460 (33) [$C_{22}H_{29}FeGaNSi^+$], 186 (100) [$C_{10}H_{10}Fe^+$]. HRMS (70 eV) *m*/*z*: calcd for $C_{32}H_{38}Fe_2GaNSi$, 645.0728; found, 645.0740. Anal. Calcd for $C_{32}H_{38}Fe_2GaNSi$ (646.15): C, 59.48; H, 5.93; N, 2.17. Found: C, 59.92; H, 6.11; N, 2.11.

Synthesis of {[Dimethyl(2-pyridyl)silyl]methyl-κ^2*C*,*N*}bis(ferrocenyl)alumane (6a). A solution of **3a** (0.49 g, 2.0 mmol) in benzene (20 mL) was added to a suspension of LiFc (0.95 g, 5.0 mmol) in benzene (30 mL). After 16 h, the precipitate was filtered off, and all volatiles were removed under vacuum. The product was extracted with hexane (105 mL) and crystallized at ca. −25 °C (0.22 g, 21%). Crystals suitable for single-crystal X-ray analysis were obtained from Et_2O solution at −25 °C. ^{1}H NMR (C_6D_6): δ −0.15 (s, 4H, CH_2), 0.37 (s, 12H, $SiMe_2$), 4.11 (m, 2H, C_5H_4), 4.15 (s, 10H, C_5H_5), 4.43 (m, 2H, C_5H_4), 4.47 (m, 4H, C_5H_4), 6.28 (m, 1H, Ar−H), 6.74 (m, 1H, Ar−H), 6.96 (m, 1H, Ar−H), 8.28 (m, 1H, Ar−H). ^{13}C NMR (C_6D_6): δ 0.72 ($SiMe_2$), 67.93 (C_5H_5), 71.18, 71.41, 75.92, 77.04 (C_5H_4), 123.87, 129.95, 137.85, 147.43, 172.22 (C_5H_4N). MS (70 eV) *m*/*z* (rel intens): 547 (15) [M^+], 187 (13) [$C_{10}H_{11}Fe^+$], 186 (100) [$C_{10}H_{10}Fe^+$], 150 (11) [$C_8H_{12}NSi^+$], 136 (24) [$C_7H_{10}NSi^+$], 121 (30) [$C_7H_6NSi^+$]. HRMS (70 eV) *m*/*z*: calcd for $C_{28}H_{30}Fe_2GaNSi$, 547.0662; found, 547.0665. Anal. Calcd for $C_{28}H_{30}AlFe_2NSi$ (547.30): C, 61.45; H, 5.52; N, 2.56. Found: C, 59.90; H, 6.56; N, 2.26.

Synthesis of {[Dimethyl(2-pyridyl)silyl]methyl-κ^2*C*,*N*}bis(ferrocenyl)gallane (6b). Species **3b** (0.61 g, 2.1 mmol) and LiFc (1.00 g, 5.21 mmol) were stirred for two days in a mixture of hexane (100 mL) and Et_2O (30 mL). After the removal of a part of the solvent (ca. 30 mL) in vacuum, the precipitate was filtered off and washed with hexane (3 × 10 mL). The volume of the solution was reduced in vacuum. Upon cooling to −25 °C a small amount of an orange colored material deposited on the walls of the flask. The mother liquor was syringed off; cooling at −78 °C resulted in an orange colored precipitate, which was separated and washed with hexane (15 and 10 mL) at −78 °C. All volatiles were removed in vacuum at ambient temperature to leave product **6b** behind (0.41 g, 33%). ^{1}H NMR (C_6D_6): δ 0.05 (s, 2H, CH_2), 0.38 (s, 6H, $SiMe_2$), 4.10 (m, 2H, C_5H_4), 4.17 (s, 10H, C_5H_5), 4.37 (m, 2H, C_5H_4), 4.44 (m, 2H, C_5H_4), 4.50 (m, 2H, C_5H_4), 6.29 (m, 1H, Ar−H), 6.76 (m, 1H, Ar−H), 6.97 (m, 1H, Ar−H), 8.18 (m, 1H, Ar−H). ^{13}C NMR (C_6D_6) δ −9.99 (CH_2), 0.58 ($SiMe_2$), 68.03 (C_5H_5), 70.58, 70.79, 75.00, 75.88, 76.12 (C_5H_4), 123.96, 129.58, 136.98, 147.55, 170.07 (C_5H_4N). MS (70 eV) *m*/*z* (rel intens): 589 (100) [M^+], 404 (75) [$M^+ - C_{10}H_9Fe$], 69 (12) [Ga^+]. HRMS (70 eV) *m*/*z*: calcd for $C_{28}H_{30}Fe_2AlNSi$, 589.0102; found, 589.0119. Anal. Calcd for $C_{28}H_{30}Fe_2GaNSi$ (590.04): C, 57.00; H, 5.12; N, 2.37. Found: C, 56.65; H, 5.05; N, 2.44.

Synthesis of Bis(ferrocenyl)dimethylsilane (7^{Me}). A solution of Me_2SiCl_2 (0.515 g, 3.99 mmol) in hexane (40 mL) was added dropwise via tubing to a slurry of LiFc (1.93 g, 10.1 mmol) in a mixture of hexane (15 mL) and Et_2O (10 mL) at r.t. The resulting reaction mixture was stirred for 16 h, yielding a red solution with orange precipitate. After the solid was filtered off, the red solution was concentrated to approximately 10 mL and kept at ca. −25 °C for 16 h. Red crystals were obtained as pure product (1.19 g, 70%). ^{1}H NMR (C_6D_6): δ 0.50 (s, 6H, CH_3), 4.02 (s, 10H, C_5H_5), 4.08, 4.19 (pst, 8H, C_5H_4). ^{13}C NMR (C_6D_6): δ −0.60 (CH_3), 68.58 (C_5H_5), 71.10, 71.62, 73.45 (C_5H_4). MS (70 eV) *m*/*z* (rel intens): 428 (100) [M^+], 363 (32) [$M^+ - C_5H_5$], 242 (9) [$M^+ - C_{10}H_{10}Fe$], 186 (8) [$C_{10}H_{10}Fe^+$]. HRMS (70 eV) *m*/*z*: calcd for $C_{22}H_{24}Fe_2Si$, 428.0346; found, 428.0361. Anal. Calcd for $C_{22}H_{24}Fe_2Si$ (428.20): C, 61.71; H, 5.65. Found: C, 61.53; H, 5.53.

Synthesis of Diethylbis(ferrocenyl)silane (7^{Et}). A solution of Et_2SiCl_2 (0.631 g, 4.02 mmol) in hexane (40 mL) was added dropwise via tubing to a slurry of LiFc (1.93 g, 10.1 mmol) in a mixture of hexane (15 mL) and Et_2O (10 mL) at r.t. The resulting reaction mixture was stirred for 16 h, yielding a red solution with orange precipitate. After the solid was filtered off, the red solution was concentrated to approximately 10 mL and kept at ca. −25 °C for 16 h. Red crystals (1.31 g, 72%) were obtained as pure product. ^{1}H NMR (C_6D_6): δ 0.99 (q, 4H, CH_2), 1.18 (t, 6H, CH_3), 4.02 (s, 10H, C_5H_5), 4.11, 4.21 (pst, 8H, C_5H_4). ^{13}C NMR (C_6D_6): δ 6.53 (CH_2), 8.44 (CH_3), 68.68 (C_5H_5), 69.75, 70.92, 73.87 (C_5H_4). MS (70 eV) *m*/*z* (rel intens): 456 (100) [M^+], 427 (38) [M^+ − Et], 333 (9) [$C_{15}H_{13}Fe_2Si^+$], 213 (30) [$C_{10}H_9FeSi^+$]. HRMS (70 eV) *m*/*z*: calcd for $C_{24}H_{28}Fe_2Si$, 456.0659; found, 456.0664. Anal. Calcd for $C_{24}H_{28}Fe_2Si$ (456.25): C, 63.18; H, 6.19. Found: C, 63.12; H, 6.19.

Single-Crystal X-ray Analysis of 3b, 6a, 7^{Me}, and 7^{Et}. Data was collected with an STOE IPDS-2 or IPDS-2T diffractometer with graphite-monochromated Mo K_α radiation (λ = 0.71073 Å) using an oil-coated schock-cooled crystal at 100 K. Absorption effects were corrected semiempirical using multiscanned reflections (PLATON).[53] Cell constants were refined using many thousands of observed reflections of the data collections.[54] The structures were solved by direct methods by using the programs SIR2008[55] (**6a**, **3b**), SIR92[56] (**7^{Me}**), or SIR97[57] (**7^{Et}**), and refined by full matrix least-squares procedures on F^2 using SHELXL-97.[58] The non-hydrogen atoms have been refined anisotropically; hydrogen atoms were included at calculated positions and refined using the "riding model" with isotropic temperature factors at 1.2 times (for CH_3 groups 1.5 times) that of the preceding carbon atom. CH_3 groups were allowed to rotate about the bond to their next atom to fit the electron density.

Compound **6a** happened to be a nonmerohedral twin with twin law [−1 0 0 0 1 0 0 0 −1]. Only the undistorted data of one twin domain have been used for the refinement (completeness of the data set 74%). Because of this twinning and the small size of the crystal the overall intensity of the data was low. During the refinement of **6a** restraints were included for the anisotropic temperature factors.

Single-Crystal X-ray Analysis of 4a and 4b. Single crystals of **4a**·2thf and **4b**·2thf were coated with Paratone-N oil, mounted using a Micromount (MiTeGen - Microtechnologies for Structural Genomics), and frozen in the cold stream of the Oxford cryojet attached to the diffractometer. Crystal data were collected at 173 K on a Bruker-AXS Proteum R Smart 6000 diffractometer using monochromated Cu K_α radiation (λ = 1.54184 Å). An initial orientation matrix and cell was determined from ω scans, and the X-ray data were measured using φ and ω scans.[59] Data reduction was performed using SAINT[60] included in the APEX2 software package.[59] A multiscan absorption correction was applied (SADABS).[58] Structures were solved by direct methods (SIR-2004)[61] and refined by full-matrix least-squares methods on F^2 with SHELX-97.[58] Unless otherwise stated, the non-hydrogen atoms were refined anisotropically; hydrogen atoms were included at geometrically idealized positions but not refined. The isotropic thermal parameters of the hydrogen atoms were fixed at 1.2 times that of the preceding carbon atom.

All thermal ellipsoid plots were prepared using ORTEP-3 for Windows.[62]

■ ASSOCIATED CONTENT

Ⓢ Supporting Information

Crystallographic data for **3b**, **4a**, **4b**, **6a**, **7^{Me}**, and **7^{Et}** in CIF file format; NMR spectra of **2a**, **3a**, **3b**, **4a**, **4b**, **5a**, **5b**, **6a**, **6b**, **7^{Me}**, and **7^{Et}**; CVs of **1a**, **4a**, **4b**, **5a**, **5b**, **6a**, **6b**, **7^{Me}**, **7^{Et}**, **8a**, and **8b**. This material is available free of charge via the Internet at http://pubs.acs.org. Crystallographic data has been deposited with the Cambridge Crystallographic Data Centre under CCDC 895302 (**3b**), 895306 (**4a**), 895307 (**4b**), 895303 (**6a**), 895304 (**7^{Me}**), and 895305 (**7^{Et}**). Copies of this information may be obtained free of charge from The Director, CCDC, 12 Union Road, Cambridge CB2 1EZ, U.K. (fax, +44−1223−336033; e-mail, deposit@ccdc.cam.ac.uk; web, http://www.ccdc.cam.ac.uk).

■ AUTHOR INFORMATION

Corresponding Author

*E-mail: jens.mueller@usask.ca.

Notes

The authors declare no competing financial interest.

■ ACKNOWLEDGMENTS

We thank the Natural Sciences and Engineering Research Council (NSERC) of Canada for a Discovery Grant (J.M.). We thank the Canada Foundation for Innovation (CFI) and the government of Saskatchewan for funding of the NMR and XRD facilities in the Saskatchewan Structural Sciences Centre (SSSC). We thank Dr. C. L. Lund (LANXESS, London, ON) and Dr. P. P. Jana (Lund University, Lund, Sweden) for contributions.

■ REFERENCES

(1) (a) Bellas, V.; Rehahn, M. *Angew. Chem., Int. Ed.* **2007**, *46*, 5082−5104. (b) Herbert, D. E.; Mayer, U. F. J.; Manners, I. *Angew. Chem., Int. Ed.* **2007**, *46*, 5060−5081.

(2) Rinehart, K. L.; Frerichs, A. K.; Kittle, P. A.; Westman, L. F.; Gustafson, D. H.; Pruett, R. L.; McMahon, J. E. *J. Am. Chem. Soc.* **1960**, *82*, 4111−4112.

(3) Osborne, A. G.; Whiteley, R. H. *J. Organomet. Chem.* **1975**, *101*, C27−C28.

(4) Foucher, D. A.; Tang, B.-Z.; Manners, I. *J. Am. Chem. Soc.* **1992**, *114*, 6246−6248.

(5) Selected recent examples: (a) Korczagin, I.; Hempenius, M. A.; Fokkink, R. G.; Stuart, M. A. C.; Al-Hussein, M.; Bomans, P. H. H.; Frederik, P. M.; Vancso, G. J. *Macromolecules* **2006**, *39*, 2306−2315. (b) Wang, X. S.; Guerin, G.; Wang, H.; Wang, Y. S.; Manners, I.; Winnik, M. A. *Science* **2007**, *317*, 644−647. (c) Gädt, T.; Ieong, N. S.; Cambridge, G.; Winnik, M. A.; Manners, I. *Nat. Mater.* **2009**, *8*, 144−150. (d) Gilroy, J. B.; Gädt, T.; Whittell, G. R.; Chabanne, L.; Mitchels, J. M.; Richardson, R. M.; Winnik, M. A.; Manners, I. *Nat. Chem.* **2010**, *2*, 566−570. (e) Presa Soto, A.; Gilroy, J. B.; Winnik, M. A.; Manners, I. *Angew. Chem., Int. Ed.* **2010**, *49*, 8220−8223. (f) Gädt, T.; Schacher, F. H.; McGrath, N.; Winnik, M. A.; Manners, I. *Macromolecules* **2011**, *44*, 3777−3786. (g) Gilroy, J. B.; Patra, S. K.; Mitchels, J. M.; Winnik, M. A.; Manners, I. *Angew. Chem., Int. Ed.* **2011**, *50*, 5851−5855. (h) He, F.; Gädt, T.; Manners, I.; Winnik, M. A. *J. Am. Chem. Soc.* **2011**, *133*, 9095−9103. (i) Patra, S. K.; Ahmed, R.; Whittell, G. R.; Lunn, D. J.; Dunphy, E. L.; Winnik, M. A.; Manners, I. *J. Am. Chem. Soc.* **2011**, *133*, 8842−8845. (j) Yusoff, S. F. M.; Hsiao, M. S.; Schacher, F. H.; Winnik, M. A.; Manners, I. *Macromolecules* **2012**, *45*, 3883−3891. (k) Rupar, P. A.; Chabanne, L.; Winnik, M. A.; Manners, I. *Science* **2012**, *337*, 559−562.

(6) Nesmeyanov, A. N.; Kritskaya, I. I. *Bull. Acad. Sci. USSR, Div. Chem. Sci. (Eng. Transl.)* **1956**, 243−244.

(7) Scheibitz, M.; Winter, R. F.; Bolte, M.; Lerner, H.-W.; Wagner, M. *Angew. Chem., Int. Ed.* **2003**, *42*, 924−927.

(8) (a) Braunschweig, H.; Burschka, C.; Clentsmith, G. K. B.; Kupfer, T.; Radacki, K. *Inorg. Chem.* **2005**, *44*, 4906−4908. (b) Schachner, J. A.; Orlowski, G. A.; Quail, J. W.; Kraatz, H.-B.; Müller, J. *Inorg. Chem.* **2006**, *45*, 454−459. (c) Schachner, J. A.; Lund, C. L.; Quail, J. W.; Müller, J. *Acta Crystallogr.* **2005**, *E61*, m682−m684.

(9) (a) Uhl, W.; Hahn, I.; Jantschak, A.; Spies, T. *J. Organomet. Chem.* **2001**, *637*, 300−303. (b) Jutzi, P.; Lenze, N.; Neumann, B.; Stammler, H. G. *Angew. Chem., Int. Ed.* **2001**, *40*, 1423−1427. (c) Althoff, A.; Jutzi, P.; Lenze, N.; Neumann, B.; Stammler, A.; Stammler, H.-G. *Organometallics* **2002**, *21*, 3018−3022. (d) Althoff, A.; Jutzi, P.; Lenze, N.; Neumann, B.; Stammler, A.; Stammler, H. G. *Organometallics* **2003**, *22*, 2766−2774.

(10) Schachner, J. A.; Lund, C. L.; Burgess, I. J.; Quail, J. W.; Schatte, G.; Müller, J. *Organometallics* **2008**, *27*, 4703−4710.

(11) (a) Herberhold, M.; Bärtl, T. *Z. Naturforsch. B* **1995**, *50*, 1692−1698. (b) Park, J. W.; Seo, Y. S.; Cho, S. S.; Whang, D. M.; Kim, K. M.; Chang, T. Y. *J. Organomet. Chem.* **1995**, *489*, 23−25. (c) Zechel, D. L.; Foucher, D. A.; Pudelski, J. K.; Yap, G. P. A.; Rheingold, A. L.; Manners, I. *J. Chem. Soc., Dalton Trans.* **1995**, 1893−1899. (d) Ni, Y. Z.; Rulkens, R.; Pudelski, J. K.; Manners, I. *Macromol. Rapid Commun.* **1995**, *16*, 637−641. (e) Reddy, N. P.; Choi, N.; Shimada, S.; Tanaka, M. *Chem. Lett.* **1996**, 649−650. (f) MacLachlan, M. J.; Zheng, J.;

Thieme, K.; Lough, A. J.; Manners, I.; Mordas, C.; LeSuer, R.; Geiger, W. E.; Liable-Sands, L. M.; Rheingold, A. L. *Polyhedron* **2000**, *19*, 275−289. (g) Calleja, G.; Carré, F.; Cerveau, G. *Organometallics* **2001**, *20*, 4211−4215. (h) Berenbaum, A.; Lough, A. J.; Manners, I. *Organometallics* **2002**, *21*, 4415−4424. (i) Bao, M.; Hatanaka, Y.; Shimada, S. *Chem. Lett.* **2004**, *33*, 520−521.

(12) (a) Seyferth, D.; Withers, H. P. *Organometallics* **1982**, *1*, 1275−1282. (b) Dong, T. Y.; Hwang, M. Y.; Wen, Y. S.; Hwang, W. S. *J. Organomet. Chem.* **1990**, *391*, 377−385. (c) Jäkle, F.; Rulkens, R.; Zech, G.; Foucher, D. A.; Lough, A. J.; Manners, I. *Chem.—Eur. J.* **1998**, *4*, 2117−2128. (d) Jäkle, F.; Rulkens, R.; Zech, G.; Massey, J.; Manners, I. *J. Am. Chem. Soc.* **2000**, *122*, 4231−4232. (e) Baumgartner, T.; Jäkle, F.; Rulkens, R.; Zech, G.; Lough, A. J.; Manners, I. *J. Am. Chem. Soc.* **2002**, *124*, 10062−10070.

(13) Utri, G.; Schwarzhans, K. E.; Allmaier, G. M. *Z. Naturforsch. B* **1990**, *45*, 755−762.

(14) (a) Brunner, H.; Klankermayer, J.; Zabel, M. *J. Organomet. Chem.* **2000**, *601*, 211−219. (b) Mizuta, T.; Onishi, M.; Miyoshi, K. *Organometallics* **2000**, *19*, 5005−5009. (c) Mizuta, T.; Imamura, Y.; Miyoshi, K. *Organometallics* **2005**, *24*, 990−996.

(15) Spang, C.; Edelmann, F. T.; Noltemeyer, M.; Roesky, H. W. *Chem. Ber.* **1989**, *122*, 1247−1254.

(16) Ieong, N. S.; Chan, W. Y.; Lough, A. J.; Haddow, M. R.; Manners, I. *Chem.—Eur. J.* **2008**, *14*, 1253−1263.

(17) Perucha, A. S.; Heilmann-Brohl, J.; Bolte, M.; Lerner, H. W.; Wagner, M. *Organometallics* **2008**, *27*, 6170−6177.

(18) (a) Lemenovskii, D. A.; Urazowski, I. F.; Baukova, T. V.; Arkhipov, I. L.; Stukan, R. A.; Perevalova, E. G. *J. Organomet. Chem.* **1984**, *264*, 283−288. (b) Kuz'mina, L. G.; Struchkov, Y. T.; Lemenovsky, D. A.; Urazowsky, I. F. *J. Organomet. Chem.* **1984**, *277*, 147−151.

(19) (a) Bagh, B.; Breit, N. C.; Gilroy, J. B.; Schatte, G.; Müller, J. *Chem. Commun.* **2012**, *48*, 7823−7825. (b) Bagh, B.; Breit, N. C.; Dey, S.; Gilroy, J. B.; Schatte, G.; Harms, K.; Müller, J. *Chem.—Eur. J.* **2012**, *18*, 9722−9733.

(20) For example: (a) Katz, T. J.; Acton, N.; Martin, G. *J. Am. Chem. Soc.* **1969**, *91*, 2804−2805. (b) Lippard, S. J.; Martin, G. *J. Am. Chem. Soc.* **1970**, *92*, 7291−7296. (c) Mueller-Westerhoff, U. T. *Angew. Chem., Int. Ed.* **1986**, *25*, 702−717. (d) Barlow, S.; Ohare, D. *Organometallics* **1996**, *15*, 3885−3890. (e) Grossmann, B.; Heinze, J.; Herdtweck, E.; Köhler, F. H.; Nöth, H.; Schwenk, H.; Spiegler, M.; Wachter, W.; Weber, B. *Angew. Chem., Int. Ed. Engl.* **1997**, *36*, 387−389. (f) Temple, K.; Lough, A. J.; Sheridan, J. B.; Manners, I. *J. Chem. Soc., Dalton Trans.* **1998**, 2799−2805. (g) Haberhauer, G.; Rominger, F.; Gleiter, R. *Angew. Chem., Int. Ed.* **1998**, *37*, 3376−3377. (h) Mueller-Westerhoff, U. T.; Swiegers, G. F. *Chem. Lett.* **1994**, 67−68. (i) Köhler, F. H.; Schell, A.; Weber, B. *Chem.—Eur. J.* **2002**, *8*, 5219−5227. (j) Schaller, R. J.; Gleiter, R.; Hofmann, J.; Rominger, F. *Angew. Chem., Int. Ed.* **2002**, *41*, 1181−1183. (k) Mizuta, T.; Aotani, T.; Imamura, Y.; Kubo, K.; Miyoshi, K. *Organometallics* **2008**, *27*, 2457−2463. (l) Herbert, D. E.; Gilroy, J. B.; Chan, W. Y.; Chabanne, L.; Staubitz, A.; Lough, A. J.; Manners, I. *J. Am. Chem. Soc.* **2009**, *131*, 14958−14968.

(21) For ferrocenophanes with more than two fc units a different nomenclature is commonly used; e.g. a FCP with 4 fc units and single-atom bridges is usually referred to as a $[1^4]$FCP instead of a [1.1.1.1] FCP (see reference 20a).

(22) (a) Bagh, B.; Schatte, G.; Green, J. C.; Müller, J. *J. Am. Chem. Soc.* **2012**, *134*, 7924−7936. (b) Breit, N. C.; Ancelet, T.; Quail, J. W.; Schatte, G.; Müller, J. *Organometallics* **2011**, *30*, 6150−6158. (c) Bagh, B.; Gilroy, J. B.; Staubitz, A.; Müller, J. *J. Am. Chem. Soc.* **2010**, *132*, 1794−1795. (d) Schachner, J. A.; Tockner, S.; Lund, C. L.; Quail, J. W.; Rehahn, M.; Müller, J. *Organometallics* **2007**, *26*, 4658−4662. (e) Lund, C. L.; Schachner, J. A.; Quail, J. W.; Müller, J. *J. Am. Chem. Soc.* **2007**, *129*, 9313−9320. (f) Lund, C. L.; Schachner, J. A.; Quail, J. W.; Müller, J. *Organometallics* **2006**, *25*, 5817−5823. (g) Schachner, J. A.; Lund, C. L.; Quail, J. W.; Müller, J. *Organometallics* **2005**, *24*, 4483−4488. (h) Schachner, J. A.; Lund, C. L.; Quail, J. W.; Müller, J. *Organometallics* **2005**, *24*, 785−787.

(23) Lund, C. L.; Schachner, J. A.; Burgess, I. J.; Quail, J. W.; Schatte, G.; Müller, J. *Inorg. Chem.* **2008**, *47*, 5992−6000.

(24) Mpysm stands for [dimethyl(2-pyridyl)silyl]methyl.

(25) Synthesis of **2b**, which was applied for the preparation the first silagalla[1.1]ferrocenophane, is described in reference 19a.

(26) All 16 H atoms at the C_5H_4 groups of **4a** or **4b** can only be in special positions (not on a symmetry element); hence, the finding of 4 signals shows a point-group symmetry with the group order of $h = 4$ (number of detected signals: $16/h = 4$).

(27) Measured chemical shifts of the four [1.1]FCPs are very similar: δ 4.01, 4.46, 4.60, 5.30 (**4a**) and 4.03, 4.40, 4.58, 5.22 (**4b**) compared with δ 4.10, 4.55, 4.64, 5.30 (**1a**) and 3.99, 4.37, 4.48, 5.07 (**1b**); see references 8a and 8b.

(28) Rosenberg, H. U.S. Patent US3426053A, 1969.

(29) Bildstein, B.; Malaun, M.; Kopacka, H.; Wurst, K.; Mitterbock, M.; Ongania, K.-H.; Opromolla, G.; Zanello, P. *Organometallics* **1999**, *18*, 4325−4336.

(30) Rulkens, R.; Lough, A. J.; Manners, I.; Lovelace, S. R.; Grant, C.; Geiger, W. E. *J. Am. Chem. Soc.* **1996**, *118*, 12683−12695.

(31) The molecular structure of 7^{Me} is mentioned in reference Andrianov, V. I. *Kristallografiya* **1987**, *32*, 1258−1260; *Sov. Phys. Crystallogr.* **1987**, *32*, 742−744 . However, besides cell parameters, structural data was not published.

(32) Scheibitz, M.; Bolte, M.; Bats, J. W.; Lerner, H. W.; Nowik, I.; Herber, R. H.; Krapp, A.; Lein, M.; Holthausen, M. C.; Wagner, M. *Chem.—Eur. J.* **2005**, *11*, 584−603.

(33) The dip angle α^* is similarly defined as the angle β in metallacyclophanes.

(34) Appel, A.; Jäkle, F.; Priermeier, T.; Schmid, R.; Wagner, M. *Organometallics* **1996**, *15*, 1188−1194.

(35) (a) Muther, K.; Fröhlich, R.; Muck-Lichtenfeld, C.; Grimme, S.; Oestreich, M. *J. Am. Chem. Soc.* **2011**, *133*, 12442−12444. (b) Schmidt, R. K.; Muther, K.; Muck-Lichtenfeld, C.; Grimme, S.; Oestreich, M. *J. Am. Chem. Soc.* **2012**, *134*, 4421−4428.

(36) Behrens, U. *J. Organomet. Chem.* **1979**, *182*, 89−98.

(37) Gleiter, R.; Bleiholder, C.; Rominger, F. *Organometallics* **2007**, *26*, 4850−4859 and cited references.

(38) Silicon species 7^{Me} and 7^{Et} were also investigated using MeCN as a solvent (see Supporting Information).

(39) Bard, A. J.; Faulkner, L. R. *Electrochemical Methods*; 2nd ed.; John Wiley & Sons, Inc.: New York, 2001.

(40) Barrière, F.; Camire, N.; Geiger, W. E.; Mueller-Westerhoff, U. T.; Sanders, R. *J. Am. Chem. Soc.* **2002**, *124*, 7262−7263.

(41) Barrière, F.; Geiger, W. E. *J. Am. Chem. Soc.* **2006**, *128*, 3980−3989.

(42) (a) Gutmann, V. *Electrochim. Acta* **1976**, *21*, 661−670. (b) Linert, W.; Fukuda, Y.; Camard, A. *Coord. Chem. Rev.* **2001**, *218*, 113−152.

(43) Additonal references on solvent effects on $\Delta E^{\circ\prime}$ values: (a) Neyhart, G. A.; Hupp, J. T.; Curtis, J. C.; Timpson, C. J.; Meyer, T. J. *J. Am. Chem. Soc.* **1996**, *118*, 3724−3729. (b) Glöckle, M.; Kaim, W. *Angew. Chem., Int. Ed.* **1999**, *38*, 3072−3074.

(44) Some CVs of bis(ferrocenyl) species using thf as a solvent exhibit weak shoulders on the main waves indicative of overlap of waves (see Supporting Information).

(45) Holleman, A. F.; Wiberg, E. *Inorganic Chemistry*, 1st English ed.; Academic Press: San Diego, CA, 2001.

(46) Jones, S. C.; Barlow, S.; O'Hare, D. *Chem.—Eur. J.* **2005**, *11*, 4473−4481.

(47) Bocarsly, A. B.; Walton, E. G.; Bradley, M. G.; Wrighton, M. S. *J. Electroanal. Chem.* **1979**, *100*, 283−306.

(48) (a) Atwood, J. L.; Bailey, B. L.; Kindberg, B. L.; Cook, W. J. *Aust. J. Chem.* **1973**, *26*, 2297−2298. (b) Atwood, J. L.; Shoemaker, A. L. *Chem. Commun.* **1976**, 536−537. (c) Rogers, R. D.; Cook, W. J.; Atwood, J. L. *Inorg. Chem.* **1979**, *18*, 279−282. (d) Robinson, G. H.; Bott, S. G.; Atwood, J. L. *J. Coord. Chem.* **1987**, *16*, 219−224. (e) Lee, B.; Pennington, W. T.; Laske, J. A.; Robinson, G. H. *Organometallics* **1990**, *9*, 2864−2865. (f) Wrackmeyer, B.; Klimkina, E. V.; Ackermann, T.; Milius, W. *Inorg. Chem. Commun.* **2007**, *10*, 743−747.

(g) Wrackmeyer, B.; Klimkina, E. V.; Milius, W. *Eur. J. Inorg. Chem.* **2009**, 3155−3162. (h) Wrackmeyer, B.; Klimkina, E. V.; Ackermann, T.; Milius, W. *Inorg. Chim. Acta* **2009**, *362*, 3941−3948.
(49) Butler, I. R.; Cullen, W. R.; Ni, J.; Rettig, S. J. *Organometallics* **1985**, *4*, 2196−2201.
(50) Cook, I. B. *Aust. J. Chem.* **1989**, *42*, 1493−1518.
(51) (a) Sindelar, K.; Holubek, J.; Svatek, E.; Matousova, O.; Metysova, J.; Protiva, M. *J. Heterocycl. Chem.* **1989**, *26*, 1325−1330. (b) Nielsen, S. F.; Larsen, M.; Boesen, T.; Schonning, K.; Kromann, H. *J. Med. Chem.* **2005**, *48*, 2667−2677. (c) Wang, Z.; Masson, G.; Peiris, F. C.; Ozin, G. A.; Manners, I. *Chem.—Eur. J.* **2007**, *13*, 9372−9383.
(52) (a) Steenwinkel, P.; James, S. L.; Grove, D. M.; Veldman, N.; Spek, A. L.; van Koten, G. *Chem.—Eur. J.* **1996**, *2*, 1440−1445. (b) Kleij, A. W.; Gebbink, R.; Lutz, M.; Spek, A. L.; van Koten, G. *J. Organomet. Chem.* **2001**, *621*, 190−196.
(53) (a) Blessing, R. H. *Acta Crystallogr., Sect. A* **1995**, *51*, 33−38. (b) Spek, A. L. *Acta Crystallogr., Sect. D: Biol. Crystallogr.* **2009**, *65*, 148−155.
(54) *X-AREA and X-RED*; Stoe & Cie GmbH: Darmstadt, Germany, 2009.
(55) Burla, M. C.; Caliandro, R.; Camalli, M.; Carrozzini, B.; Cascarano, G. L.; De Caro, L.; Giacovazzo, C.; Polidori, G.; Siliqi, D.; Spagna, R. *J. Appl. Crystallogr.* **2007**, *40*, 609−613.
(56) Altomare, A.; Cascarano, G.; Giacovazzo, C.; Guagliardi, A. *J. Appl. Crystallogr.* **1993**, *26*, 343−350.
(57) Altomare, A.; Burla, M. C.; Camalli, M.; Cascarano, G.; Giacovazzo, C.; Guagliardi, A.; Moliterni, A. G. G.; Polidori, G.; Spagna, R. *J. Appl. Crystallogr.* **1999**, *32*, 115−119.
(58) Sheldrick, G. M. *Acta Crystallogr., Sect. A* **2008**, *64*, 112−122.
(59) *APEX2*; Bruker AXS Inc.: Madison, WI, 2009.
(60) *SAINT and SADABS*; Bruker AXS Inc.: Madison, WI, 2009.
(61) Burla, M. C.; Caliandro, R.; Camalli, M.; Carrozzini, B.; Cascarano, G. L.; De Caro, L.; Giacovazzo, C.; Polidori, G.; Spagna, R. *J. Appl. Crystallogr.* **2005**, *38*, 381−388.
(62) Farrugia, L. J. *J. Appl. Crystallogr.* **1997**, *30*, 565.